A Novel Approach for Model-Based Control of Smooth and Lossless Gear Shifts

Johannes Rumetshofer, Markus Bachinger, Michael Stolz, and Martin Horn, *Member, IEEE*

***Abstract*—In contrast to conventional and classical hybrid electric transmissions, multimode (hybrid electric) transmissions open new perspectives in gear shifting: The tradeoff between avoidance of propulsion torque interruption and dissipation in clutches can be resolved by smart utilization of the second, coequal, propulsion element, and rearrangement of standard shift phases (torque phase and inertia phase). The resulting smooth and lossless gear shifts reach a new level of performance combining comfort and efficiency. Therefore, modeling and control of these gear shifts is an ongoing automotive research topic since several years. However, so far there is no systematic, model-based approach, which would enable broad application in industry. This paper contributes to bridge this gap. The key point is a systematic determination of a consistent set of generalized coordinates, corresponding to a specific gear, i.e., set of locked clutches. This is achieved by exploiting the mechanical peculiarities of drivetrain topologies. Based on this, a straightforward transformation is proposed to derive a comprehensive state-space model for each gear of a given topology. This enables the statement of the control problem for smooth and lossless gear shifting in a novel compact and general form. Finally, a new shift procedure and a generic-model-based feedforward control is proposed and applied to an exemplary multimode transmission. Promising first simulation results confirm the significance of the proposed approach for further investigation and application.**

***Index Terms*—Multi-mode transmissions (MMT), gear shift control, torque control, velocity control.**

I. Introduction

THE automation of gear shifting plays an important role in increasing the energy efficiency of vehicles. The quality of gear shifting is basically evaluated considering on the one hand the impact on the propulsion torque (torque interruption, torque ripples) and on the other hand the dissipation due to friction in the clutches. In this context gear shifting is optimal, if it is performed smoothly, considering impact on the propulsion torque, and losslessly, considering dissipation in clutches. In conventional drivetrain topologies, e.g., AMT (automated manual transmission), DCT (dual clutch transmission), and AT (automatic transmission) this optimum is out of reach due to topological limitations. Therefore, shifting in these topologies always accepts a compromise between both objects, in which torque interruption obviously obtains higher attention. For different shifting control approaches in conventional transmissions the interested reader is referred to [1]–[7].

In the last two decades hybrid electric vehicles (HEV) have gained more and more importance due to the ongoing attempt to reduce emissions. A multitude of new transmission topologies and transmission classifications have been proposed and marketed. Special operating modes like fixed compound (FC) mode, also known as torque-split mode, and electric continuous variable (CV) mode, also known as power-split mode, reduce the total number of gears and clutches. Most topologies consist of one single clutch (e.g., [8]) or even do without any clutch (e.g., "THS II-like" in [9]). Therefore, although the introduction of a second propulsion element, the electric motor, allows consideration of smooth and lossless shifting, in general, shifting seemed to become less important for those topologies. The single shift, for example to decouple internal combustion engine (ICE) from the transmission is treated as a special case without any need for generalization: In [10] resp. [11] general overviews on shifting control requirements resp. control strategies for hybrid electric vehicles are given. Jerk minimization during shifting for parallel hybrid electric transmission is presented in [12]–[18].

Modern multi-mode transmissions (MMT, see [9]), however, combine different operating modes into single transmissions. At this point gear shifting in general, and smooth and lossless gear shifting in particular recapture attention. In MMTs the electric motor is applied as coequal, non redundant propulsion element. These topologies are also named dedicated hybrid transmissions (DHT, see [19]) or motor-integrated parallel hybrid electric transmission (see [20]). Furthermore series-parallel hybrid electric transmissions can be assigned to this class. In references [8] and [21] the vehicle jerk and dissipation in clutches are minimized for series-parallel hybrid electric vehicles, but still the trade-off is present. In [22] the equations of motion derived with Kanes method in terms of generalized speed components is considered and manipulated into a state space system. The presented approach considers exclusively the synchronization

Manuscript received July 5, 2017; revised September 15, 2017; accepted September 24, 2017. Date of publication October 5, 2017; date of current version February 12, 2018. This work was supported in part by the COMET K2—Competence Centres for Excellent Technologies Programme of the Austrian Federal Ministry for Transport, Innovation and Technology (bmvit), in part by the Austrian Federal Ministry of Science, Research and Economy (bmwfw), in part by the Austrian Research Promotion Agency (FFG), in part by the Province of Styria and the Styrian Business Promotion Agency (SFG). The review of this paper was coordinated by Dr. D. Cao. *(Corresponding author: Johannes Rumetshofer.)*

J. Rumetshofer and M. Stolz are with the Virtual Vehicle Research Center, Graz 8010, Austria (e-mail: johannes.rumetshofer@v2c2.at; michael.stolz@v2c2.at)

M. Bachinger is with AVL LIST GmbH, Graz 8020, Austria (e-mail: markus.bachinger@avl.com).

M. Horn is with the Institute of Automation and Control, Graz University of Technology, Graz 8010, Austria (e-mail: martin.horn@tugraz.at).

Color versions of one or more of the figures in this paper are available online at http://ieeexplore.ieee.org.

Digital Object Identifier 10.1109/TVT.2017.2759321

of a clutch. Summarized, smooth and lossless gear shifting has already been considered in many partial aspects, but there is still no systematic, general, model-based approach.

In this paper Chapter II contains detailed linear drivetrain modeling based on classical multibody mechanics. Key point is the determination of a set of generalized coordinates (c.f. generalized speed components in [22]). This determination enables simple transformation from one state space model considering all clutches to be slipping to all (sub) state space models for all possible gears, i.e., sets of locked clutches. This transformation furthermore achieves a description of the general control tasks (synchronizing or unloading a clutch while delivering required propulsion torque) in state space (see Chapter III). Since the task is to control two system outputs independently by employing two system inputs, the question, if a specific gear shift in a given drivetrain topology can be performed in the required way, leads to a decoupling problem. Decoupling theory is used to give a sufficient condition to perform smooth and loss less gear shifts. If this condition is met the general representation as a MIMO (multi-input-multi-output) tracking problem facilitates the application of standard control strategies.

Finally, all general preliminary investigations are applied to an exemplary MMT in Chapter IV, including the linear modeling approach, the formulation of the tracking resp. decoupling problem, and the evaluation of possible gear shifts. A generic, model-based feedforward control strategy is proposed to perform exemplary smooth and lossless gear shifts applying a novel shift procedure. A multi clutch actuation is avoided and clutch transitions (slip to lock or lock to slip), which are the most critical point in standard shifting procedures, do not cause big difficulties anymore.

The control strategy is evaluated in first simulations in combination with an already validated drivetrain model [23].

II. Drivetrain Modeling

Drivetrain modeling has been covered in several publications (e.g., [1] and [23]). It forms the mathematical basis of the ideas presented in this paper. Therefore, it is considered in detail in this section. The task is to deduce a state space model describing the drivetrain's dynamical behavior. This dynamical behavior is defined by the rotational motion of inertias and the interaction between them. From the mechanical point of view a drivetrain topology classifies as follows:

1) dynamic multibody system
2) one rotational degree of freedom per inertia
3) additional holonomic constraints due to locked clutches.

The unconstrained equations of motion of inertias are defined in Newton's laws of motion. D'Alembert's principle and Lagrange formalism (see for example [24] and [25]) determine the impact of locked clutches. This standard approach in classical mechanics is now applied in drivetrain modeling in detail similar to [1]. Given a linear state space model of a drivetrain topology, which considers all clutches to be slipping, this chapter gives a compact approach to select a set of generalized coordinates and transform the state space model in case of one or several locked clutches.

A. Unconstrained Equations of Motion

According to Newton's laws of motion, the dynamics of a multibody system is represented in a system of ordinary differential equations of second order with respect to the inertias' positions. Since there is only one single rotational degree of freedom per inertia, these positions are defined by a vector of angular positions $\boldsymbol{\varphi}$. The restriction to linear position resp. velocity dependent forces leads to a linear system of ordinary differential equations second order:

$$\mathbf{M}\ddot{\boldsymbol{\varphi}} = -\mathbf{D}\dot{\boldsymbol{\varphi}} - \mathbf{K}\boldsymbol{\varphi} + \boldsymbol{\tau}. \tag{1}$$

$\mathbf{M}$ denotes the inertia or mass matrix, being diagonal and positive definite. Assuming every motion to be affected by kinetic friction, the so called damping matrix $\mathbf{D}$ is a positive definite matrix. Stiffness matrix $\mathbf{K}$ is a positive semidefinite matrix. $\mathbf{K}$ together with $\mathbf{D}$ define the interaction between inertias via flexible shafts. The vector $\boldsymbol{\tau}$ contains all external, i.e., position and velocity independent, torques. The vector of external torques $\boldsymbol{\tau}$ can be replaced by a linear mapping $\hat{\mathbf{B}}$ of all considered input torques $\mathbf{u}$. In drivetrain modeling these input torques are divided into propulsion torques $\boldsymbol{\tau}_{\mathrm{P}}$, vehicle reaction torque τ_{V} (due to road gradient, rolling resistance, and air drag), and clutch torques $\boldsymbol{\tau}_{\mathrm{C}}$:

$$\boldsymbol{\tau} = \hat{\mathbf{B}}\mathbf{u}, \qquad \mathbf{u}^T = \begin{bmatrix} \boldsymbol{\tau}_{\mathrm{P}}^T & \tau_{\mathrm{V}} & \boldsymbol{\tau}_{\mathrm{C}}^T \end{bmatrix}. \tag{2}$$

Note that τ_{V} is considered a disturbance input. The definition of a state vector $\hat{\mathbf{x}}^T = \begin{bmatrix} \boldsymbol{\varphi}^T & \dot{\boldsymbol{\varphi}}^T \end{bmatrix}$ consisting of both angular positions $\boldsymbol{\varphi}$ and velocities $\dot{\boldsymbol{\varphi}}$ transforms (1) into a system of ordinary linear differential equations first order:

$$\begin{bmatrix} \mathbf{I} & \mathbf{0} \\ \mathbf{0} & \mathbf{M} \end{bmatrix} \dot{\hat{\mathbf{x}}} = \begin{bmatrix} \mathbf{0} & \mathbf{I} \\ -\mathbf{K} & -\mathbf{D} \end{bmatrix} \hat{\mathbf{x}} + \begin{bmatrix} \mathbf{0} \\ \hat{\mathbf{B}} \end{bmatrix} \mathbf{u}. \tag{3}$$

$\mathbf{I}$ denotes an identity matrix of appropriate dimension. In drivetrain modeling angular velocities represent the matter of interest in drivetrain modeling. Therefore, equations concerning angular positions, which are not influenced by position dependent torques, i.e., spring torques, can be omitted. The number of states assigned to the remaining angular positions can be further reduced by combining them to spring torsions, i.e., the differential angular positions $\Delta\boldsymbol{\varphi}$ of inertias connected via a flexible shaft. Considering a number of N inertias and g flexible shafts, this modification leads to a system Σ of $n = N + g$ ordinary linear differential equations of first order,

$$\Sigma : \bar{\mathbf{M}}\dot{\mathbf{x}} = \bar{\mathbf{A}}\mathbf{x} + \bar{\mathbf{B}}\mathbf{u}, \quad \text{with} \quad \mathbf{x}^T = \begin{bmatrix} \dot{\boldsymbol{\varphi}}^T & \Delta\boldsymbol{\varphi}^T \end{bmatrix}. \tag{4}$$

The dimension of $\mathbf{x}$ is minimal with respect to the interests in drivetrain modeling. According to the separation of the input torques in (2), the input matrix $\bar{\mathbf{B}}$ consists of three parts:

$$\bar{\mathbf{B}} = \begin{bmatrix} \bar{\mathbf{B}}_{\mathrm{P}}, \bar{\boldsymbol{b}}_{\mathrm{V}}, \bar{\mathbf{B}}_{\mathrm{C}} \end{bmatrix}. \tag{5}$$

Since matrix $\bar{\mathbf{M}}$ is non singular [see (3) and remarks on (1)], left multiplication by the inverse matrix $\bar{\mathbf{M}}^{-1}$ leads to a state space model:

$$\dot{\mathbf{x}} = \underbrace{\bar{\mathbf{M}}^{-1}\bar{\mathbf{A}}}_{\mathbf{A}}\mathbf{x} + \underbrace{\bar{\mathbf{M}}^{-1}\bar{\mathbf{B}}}_{\mathbf{B}}\mathbf{u}. \tag{6}$$

Note that the transformation from state space model (6) back to Σ (4) is not unique. Since the matrix $\bar{\mathbf{M}}$ will play a key role when investigating the impact of locked clutches, the notation of the system in (4) is of higher importance than that in (6).

B. Impact of Locked Clutches

A clutch represents a rigid shaft, if it is in locked state. Therefore, a binary variable for each clutch is introduced, stating whether the respective clutch is locked or not. These binary variables are assembled to a binary vector $\boldsymbol{\kappa}$, called clutch state vector. In a first step the impact of one locked clutch is considered. Therefore, the corresponding clutch state vector $\boldsymbol{\kappa}_i$ fulfills $\boldsymbol{\kappa}_i^T \boldsymbol{\kappa}_i = 1$. A locked clutch requires zero differential angular velocity $\Delta\dot{\varphi}_{\mathrm{C,lk}}$ between the clutch plates. In order to formulate a general holonomic constraint $f(\mathbf{x}) = 0$, the general relation between differential angular velocities between the clutch plates $\Delta\dot{\boldsymbol{\varphi}}_{\mathrm{C}}$ and states $\mathbf{x}$ is investigated. According to (4) and (5), the matrix $\bar{\mathbf{B}}_{\mathrm{C}}$ maps clutch torques to torques acting directly at the inertias. Since this mapping must not change the total power, the following identity holds:

$$\boldsymbol{\tau}_{\mathrm{C}}^T \bar{\mathbf{B}}_{\mathrm{C}}^T \mathbf{x} \equiv \boldsymbol{\tau}_{\mathrm{C}}^T \Delta\dot{\boldsymbol{\varphi}}_{\mathrm{C}}. \tag{7}$$

This determines the mapping $\mathbf{x} \mapsto \Delta\dot{\boldsymbol{\varphi}}_{\mathrm{C}}$:

$$(7) \quad \Rightarrow \quad \Delta\dot{\boldsymbol{\varphi}}_{\mathrm{C,lk}} = \bar{\mathbf{B}}_{\mathrm{C}}^T \mathbf{x} \tag{8}$$

According to (8) the constraint $f(\mathbf{x})$ due to a locked clutch is calculated by selecting the respective column of matrix $\bar{\mathbf{B}}_{\mathrm{C}}$:

$$f(\mathbf{x}) = \Delta\dot{\varphi}_{\mathrm{C}} = \bar{\mathbf{b}}_{\mathrm{C,lk}}^T \mathbf{x} \stackrel{!}{=} 0, \quad \text{with:} \quad \bar{\mathbf{b}}_{\mathrm{C,lk}} := \bar{\mathbf{B}}_{\mathrm{C}} \boldsymbol{\kappa}_i. \tag{9}$$

This constraint is indeed holonomic and furthermore linear with respect to the state $\mathbf{x}$. Due to this holonomic constraint the system loses one degree of freedom, i.e., not all inertias can move independently anymore. In Lagrange formalism the impact of a holonomic constraints on the system's dynamic is handled by introducing a constraining torque. D'Alembert's principle defines the direction of the constraining torque as

$$\nabla f(\mathbf{x}) = \left[\frac{\partial f(\mathbf{x})}{\partial \mathbf{x}}\right]^T = \bar{\mathbf{b}}_{\mathrm{C,lk}}. \tag{10}$$

The magnitude of the constraining torque is an additional variable, a so called Lagrangian multiplier λ. This leads to a linear, differential algebraic equation (DAE) system consisting of n linear, ordinary differential equations of first order and one linear, algebraic equation:

$$\bar{\mathbf{M}}\dot{\mathbf{x}} = \bar{\mathbf{A}}\mathbf{x} + \bar{\mathbf{B}}_{\mathrm{R}}\mathbf{u}_{\mathrm{R}} + \bar{\mathbf{b}}_{\mathrm{C,lk}}\lambda, \tag{11}$$

$$\bar{\mathbf{b}}_{\mathrm{C,lk}}^T \mathbf{x} = 0. \tag{12}$$

Hereby $\mathbf{u}_{\mathrm{R}}$ denotes the remaining inputs disregarding the torque $\tau_{\mathrm{C,lk}} = \boldsymbol{\kappa}_i^T \boldsymbol{\tau}_{\mathrm{C}}$ transmitted at the locked clutch, and $\bar{\mathbf{B}}_{\mathrm{R}}$ represents the corresponding columns of the original input matrix $\bar{\mathbf{B}}$. The physical meaning of λ is clarified by splitting the input vector $\mathbf{u}$ and the input matrix $\bar{\mathbf{B}}$ in the unconstrained system (4) analogously to (11):

$$\bar{\mathbf{M}}\dot{\mathbf{x}} = \bar{\mathbf{A}}\mathbf{x} + \bar{\mathbf{B}}_{\mathrm{R}}\mathbf{u}_{\mathrm{R}} + \bar{\mathbf{b}}_{\mathrm{C,lk}}\tau_{\mathrm{C,lk}} \tag{13}$$

Comparison of (13) and (11) illustrates the equivalence of the Lagrange multiplier and the clutch torque $\tau_{\mathrm{C,lk}}$:

$$\tau_{\mathrm{C,lk}} := \lambda, \tag{14}$$

Consequently, $\tau_{\mathrm{C,lk}}$ is no system input, but is determined by the state $\mathbf{x}$ and system inputs $\mathbf{u}_{\mathrm{R}}$. It is therefore called locking torque and can be calculated explicitly by derivation of the constraint in (9) and usage of (13):

$$\begin{aligned} \bar{\mathbf{b}}_{\mathrm{C,lk}}^T \dot{\mathbf{x}} &= 0 \\ \bar{\mathbf{b}}_{\mathrm{C,lk}}^T \bar{\mathbf{M}}^{-1} \left[\bar{\mathbf{A}}\mathbf{x} + \bar{\mathbf{B}}_{\mathrm{R}}\mathbf{u}_{\mathrm{R}} + \bar{\mathbf{b}}_{\mathrm{C,lk}}\tau_{\mathrm{C,lk}}\right] &= 0 \\ -\left[\bar{\mathbf{b}}_{\mathrm{C,lk}}^T \bar{\mathbf{M}}^{-1} \bar{\mathbf{b}}_{\mathrm{C,lk}}\right]^{-1} \bar{\mathbf{b}}_{\mathrm{C,lk}}^T \bar{\mathbf{M}}^{-1} \left[\bar{\mathbf{A}}\mathbf{x} + \bar{\mathbf{B}}_{\mathrm{R}}\mathbf{u}_{\mathrm{R}}\right] &= \tau_{\mathrm{C,lk}}. \end{aligned} \tag{15}$$

The disadvantage of the differential algebraic system in (11)-(12) is the need for $(n+1)$ equations to describe the dynamics of a mechanical system having $(n-1)$ degrees of freedom. Elimination of the Lagrangian multiplier resolves this disadvantage. The Lagrange formalism therefore introduces the idea of generalized coordinates $\mathbf{q}_i$. These generalized coordinates $\mathbf{q}_i$ comply with the holonomic constraint for arbitrary values:

$$\frac{\partial f}{\partial \mathbf{q}_i} = \frac{\partial f}{\partial \mathbf{x}} \frac{\partial \mathbf{x}}{\partial \mathbf{q}_i} \equiv 0, \tag{16}$$

Whereas $\partial f / \partial \mathbf{x}$ is already defined in (10), the expression $\partial \mathbf{x} / \partial \mathbf{q}_i$ introduces a new transformation $\mathbf{J}_{\mathrm{x},\mathrm{q}_i}$. Due to the linearity of the constraint it is a linear mapping:

$$\frac{\partial \mathbf{x}}{\partial \mathbf{q}_i} =: \mathbf{J}_{\mathrm{x},\mathrm{q}_i} \;\Rightarrow\; \mathbf{x} = \mathbf{J}_{\mathrm{x},\mathrm{q}_i} \mathbf{q}_i. \tag{17}$$

If $\mathbf{J}_{\mathrm{x},\mathrm{q}_i}$ is a basis of $\bar{\mathbf{b}}_{\mathrm{C,lk}}^T$'s nullspace (see for example [26]), (16) holds for arbitrary $\mathbf{q}_i$:

$$\mathbf{J}_{\mathrm{x},\mathrm{q}_i} \in \mathcal{N}\left(\bar{\mathbf{b}}_{\mathrm{C,lk}}^T\right) \;\Rightarrow\; \underbrace{\bar{\mathbf{b}}_{\mathrm{C,lk}}^T \mathbf{J}_{\mathrm{x},\mathrm{q}_i}}_{=0} \mathbf{q}_i \equiv 0. \tag{18}$$

Since the dimension of the matrix $\mathbf{J}_{\mathrm{x},\mathrm{q}_i}$ determines the number of generalized coordinates $\mathbf{q}_i$, it is considered in detail. The rank-nullity theorem (see for example [26]) determines the dimension of $\bar{\mathbf{b}}_{\mathrm{C,lk}}^T$'s nullspace:

$$\dim \mathcal{N}\left(\bar{\mathbf{b}}_{\mathrm{C,lk}}^T\right) = \dim(\mathbb{R}^n) - \dim \mathcal{R}\left(\bar{\mathbf{b}}_{\mathrm{C,lk}}^T\right) = n - 1. \tag{19}$$

($\mathcal{R}$ is the range and $\mathcal{N}$ the nullspace of a mapping.) According to (18) and the mapping $\bar{\mathbf{b}}_{\mathrm{C,lk}}^T : \mathbb{R}^n \mapsto \mathbb{R}$, the matrix $\mathbf{J}_{\mathrm{x},\mathrm{q}_i}$ is a $n \times (n-1)$-matrix and therefore the number of generalized coordinates is $(n-1)$. This number equals the system's number of mechanical degrees of freedom. Note that if $\mathbf{J}_{\mathrm{x},\mathrm{q}_i}$ is in reduced row echelon form (see for example [26]), the generalized coordinates $\mathbf{q}_i$ are a selection of the original states $\mathbf{x}$. Since (18) is the only condition for $\mathbf{J}_{\mathrm{x},\mathrm{q}_i}$, this is always possible and ensures the consistent physical meaning of the generalized coordinates $\mathbf{q}_i$ with respect to $\mathbf{x}$. Consequently, the inverse mapping $\mathbf{q}_i = \mathbf{J}_{\mathrm{q_i},\mathrm{x}}\mathbf{x}$ is a selection matrix.

Left multiplication by $\mathbf{J}_{\mathrm{x,q}_i}^T$ in (11) eliminates the Lagrangian multiplier:

$$\mathbf{J}_{\mathrm{x,q}_i}^T \bar{\mathbf{M}}\dot{\mathbf{x}} = \mathbf{J}_{\mathrm{x,q}_i}^T \bar{\mathbf{A}}\mathbf{J}_{\mathrm{x,q}_i}\mathbf{x} + \mathbf{J}_{\mathrm{x,q}_i}^T \bar{\mathbf{B}}_{\mathrm{R}}\mathbf{u}_{\mathrm{R}} + \underbrace{\mathbf{J}_{\mathrm{x,q}_i}^T \bar{\mathbf{b}}_{\mathrm{C,lk}}}_{=0}\lambda. \quad (20)$$

Furthermore, the transformation to generalized coordinates yields a new dynamical system:

$$\Sigma_{\boldsymbol{\kappa}_i} : \underbrace{\mathbf{J}_{\mathrm{x,q}_i}^T \bar{\mathbf{M}}\mathbf{J}_{\mathrm{x,q}_i}}_{\bar{\mathbf{M}}_i}\dot{\mathbf{q}}_i = \underbrace{\mathbf{J}_{\mathrm{x,q}_i}^T \bar{\mathbf{A}}\mathbf{J}_{\mathrm{x,q}_i}}_{\bar{\mathbf{A}}_i}\mathbf{q}_i + \underbrace{\mathbf{J}_{\mathrm{x,q}_i}^T \bar{\mathbf{B}}}_{\bar{\mathbf{B}}_i}\mathbf{u}. \quad (21)$$

$\Sigma_{\boldsymbol{\kappa}_i}$ consists of $(n-1)$ ordinary, linear differential equations. This number is minimal according to the system's $(n-1)$ mechanical degrees of freedom. Note that $\bar{\mathbf{B}}_i$ contains a zero column. Left-multiplication by the regular matrix $\bar{\mathbf{M}}_i^{-1}$ in (21) leads to a state space model:

$$\dot{\mathbf{q}}_i = \underbrace{\bar{\mathbf{M}}_i^{-1}\bar{\mathbf{A}}_i}_{\mathbf{A}_i}\mathbf{q}_i + \underbrace{\bar{\mathbf{M}}_i^{-1}\bar{\mathbf{B}}_i}_{\mathbf{B}_i}\mathbf{u}. \quad (22)$$

The above approach of adding one holonomic constraint can be extended to m holonomic constraints according to m locked clutches ($1 \leq m < n$). Consequently, $\boldsymbol{\kappa}_i$ contains m nonzero entries ($\boldsymbol{\kappa}_i^T\boldsymbol{\kappa}_i = m$). The vector $\bar{\mathbf{b}}_{\mathrm{C,lk}}$ is extended to an $n \times m$-matrix $\bar{\mathbf{B}}_{\mathrm{C,lk}}$, which is the selection of m columns in $\bar{\mathbf{B}}_{\mathrm{C}}$ according to $\boldsymbol{\kappa}_i$. The symbol $\bar{\mathbf{B}}_{\mathrm{C}}(\boldsymbol{\kappa}_i)$ denotes this selection of respective columns:

$$\bar{\mathbf{B}}_{\mathrm{C,lk}} := \bar{\mathbf{B}}_{\mathrm{C}}(\boldsymbol{\kappa}_i). \quad (23)$$

The vector of constraints $\mathbf{f}(\mathbf{x})$ therefore is:

$$\mathbf{f}(\mathbf{x}) = \bar{\mathbf{B}}_{\mathrm{C,lk}}\mathbf{x} \stackrel{!}{=} \mathbf{0}. \quad (24)$$

Hereby $\mathbf{0}$ is a zero matrix of dimensions $(m \times 1)$. The directions of the constraining torques are determined by the transpose of the Jacobian of the constraints:

$$\mathbf{J}_{\mathrm{f}}^T = \left[\frac{\partial \mathbf{f}(\mathbf{x})}{\partial \mathbf{x}}\right]^T = \bar{\mathbf{B}}_{\mathrm{C,lk}}. \quad (25)$$

According to (19), $\mathbf{J}_{\mathrm{x,q}_i}$ now is an $n \times (n-m)$-matrix. Consequently, the system loses m degrees of freedom. The elimination of the Lagrangian multipliers $\boldsymbol{\lambda}$ and the transformation to generalized coordinates can be applied analogously as stated in (21), which defines the relations between unconstrained and constrained system matrices $(\bar{\mathbf{M}}, \bar{\mathbf{A}}, \bar{\mathbf{B}} \mapsto \bar{\mathbf{M}}_i, \bar{\mathbf{A}}_i, \bar{\mathbf{B}}_i)$. Therefore, the dynamics of the drivetrain topology is entirely described by the mathematical model Σ considering all clutches not to be locked in (4) and the clutch state vector $\boldsymbol{\kappa}_i$. Summarized the transformed system dynamics can be computed as follows:

1) Determine $\bar{\mathbf{B}}_{\mathrm{C,lk}}$ by selecting the columns of $\bar{\mathbf{B}}_{\mathrm{C}}$ according to the nonzero entries of $\boldsymbol{\kappa}_i$, which identify the locked clutches:

$$\bar{\mathbf{B}}_{\mathrm{C,lk}} = \bar{\mathbf{B}}_{\mathrm{C}}(\boldsymbol{\kappa}_i). \quad (26)$$

2) Find a basis $\mathbf{J}_{\mathrm{x,q}_i}$ to $\bar{\mathbf{B}}_{\mathrm{C,lk}}^T$'s null space in reduced row echelon form:

$$\bar{\mathbf{B}}_{\mathrm{C,lk}}^T\mathbf{J}_{\mathrm{x,q}_i} = \mathbf{0} \quad \Rightarrow \mathbf{x} = \mathbf{J}_{\mathrm{x,q}_i}\mathbf{q}_i. \quad (27)$$

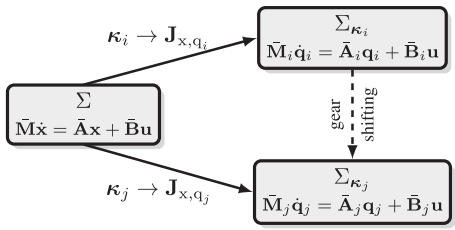

Fig. 1. Relations between the mathematical models Σ, $\Sigma_{\boldsymbol{\kappa}_i}$ and $\Sigma_{\boldsymbol{\kappa}_j}$ in a general gear shift $\boldsymbol{\kappa}_i \rightarrow \boldsymbol{\kappa}_j$ [see (4) and (26)–(28)].

3) Use $\mathbf{J}_{\mathrm{x,q}_i}$ to transform system parameters:

$$\bar{\mathbf{M}}_i = \mathbf{J}_{\mathrm{x,q}_i}^T\bar{\mathbf{M}}\mathbf{J}_{\mathrm{x,q}_i},\ \bar{\mathbf{A}}_i = \mathbf{J}_{\mathrm{x,q}_i}^T\bar{\mathbf{A}}\mathbf{J}_{\mathrm{x,q}_i},\ \bar{\mathbf{B}}_i = \mathbf{J}_{\mathrm{x,q}_i}^T\bar{\mathbf{B}}. \quad (28)$$

These three steps completely define the relation between the dynamical systems Σ and $\Sigma_{\boldsymbol{\kappa}_i}$:

$$\Sigma : \bar{\mathbf{M}}\dot{\mathbf{x}} = \bar{\mathbf{A}}\mathbf{x} + \bar{\mathbf{B}}\mathbf{u}$$
$$\Downarrow (26) - (28)$$
$$\Sigma_{\boldsymbol{\kappa}_i} : \bar{\mathbf{M}}_i\dot{\mathbf{q}}_i = \bar{\mathbf{A}}_i\mathbf{q}_i + \bar{\mathbf{B}}_i\mathbf{u}. \quad (29)$$

The respective locking torques $\boldsymbol{\tau}_{\mathrm{C,lk}}$ are determined by:

$$\boldsymbol{\tau}_{\mathrm{C,lk}} = -\left[\bar{\mathbf{B}}_{\mathrm{C,lk}}^T\bar{\mathbf{M}}^{-1}\bar{\mathbf{B}}_{\mathrm{C,lk}}\right]^{-1}\bar{\mathbf{B}}_{\mathrm{C,lk}}^T\bar{\mathbf{M}}^{-1}\left[\bar{\mathbf{A}}\mathbf{x} + \bar{\mathbf{B}}_{\mathrm{R}}\mathbf{u}_{\mathrm{R}}\right]. \quad (30)$$

Alternatively the overall impact of several locked clutches can be determined by consecutively considering the case of one single locked clutch.

C. Gear Shifting

Gear shifting is the process of locking or releasing at least one clutch in order to change the transmission mode. The process of locking resp. releasing a clutch is initiated by increasing resp. decreasing the pressure p on the clutch plates (cf., Fig. 2). In practice this is done by hydraulic actuation (see for example [27]). If $p > 0$ is applied to a released clutch, it will enter the slipping state. Due to kinetic friction a slipping torque $\tau_{\mathrm{C,sl}}$ occurs. Increasing p above a limit depending on state vector $\mathbf{x}$, the remaining inputs $\mathbf{u}_{\mathrm{R}}$, and the friction coefficients, forces the clutch into locked state. The exact conditions for this transition between slipping and locked state will be not of importance in the context of this paper, but in standard shift procedures they represent one of the most critical points. The interested reader is referred to [23]. In order to release a locked clutch, p has to be decreased to zero, forcing the clutch to enter slipping and later released state.

From the mathematical point of view gear shifting implies the transition from the current clutch state $\boldsymbol{\kappa}_i$ to a clutch state $\boldsymbol{\kappa}_j$ and consequently, according to Section II-B, the transition between two dynamical systems $\Sigma_{\boldsymbol{\kappa}_i}$ and $\Sigma_{\boldsymbol{\kappa}_j}$. Fig. 1 illustrates the relations of these systems to the unconstrained system Σ in (4). The overall system, consequently, is time varying, but due to the modeling approach piecewise linear (cf. [4]).

In the following, elementary gear shifts are considered, which allow only the change of one single clutch state (released to

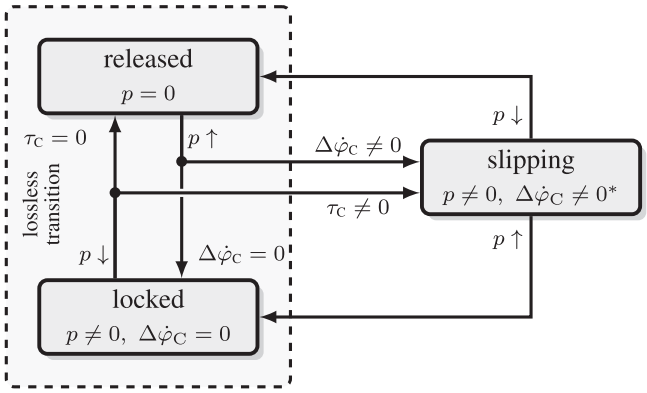

Fig. 2. Clutch states and possible transitions (τ_C clutch torque, $\Delta\dot{\varphi}_C$ differential angular velocity between the clutch plates, p pressure on the clutch plates; *The conditions of slipping state are only valid stationary).

locked resp. locked to released). The following condition ensures that the considered gear shift ($\boldsymbol{\kappa}_i \rightarrow \boldsymbol{\kappa}_j$) is elementary:

$$\Delta\boldsymbol{\kappa}_{i,j}^T \Delta\boldsymbol{\kappa}_{i,j} \stackrel{!}{=} 1, \quad \text{with:} \quad \Delta\boldsymbol{\kappa}_{i,j} := \boldsymbol{\kappa}_i \veebar \boldsymbol{\kappa}_j. \tag{31}$$

(The symbol $\veebar$ denotes the element-wise logical exclusive disjunction.) $\Delta\boldsymbol{\kappa}_{i,j}$ identifies the clutch, which is locked resp. released. This consideration is not restrictive since every non-elementary gear shift can be split into a series of elementary gear shifts. In elementary gear shifts one additional mechanical degree of freedom appears either in $\Sigma_{\boldsymbol{\kappa}_i}$ or in $\Sigma_{\boldsymbol{\kappa}_j}$. Note that since incorporation of impacts of locked clutches can be done consecutively, the parameters of the system with a lower number of mechanical degrees of freedom can be directly calculated from the parameters of the other system.

At this point it should be mentioned that this publication in a first step neglects nonlinear behavior of automotive drivetrains, which are treated in several publication (e.g., torsional vibrations caused by the backlash in the drivetrain in [28] and [29]). Being aware of the possible significance of nonlinear effects, their consideration is planned to be done after practical testing of the presented approaches, as the measurements proof the necessity.

III. Smooth and Lossless Gear Shifting in State Space

The previous chapter presented a mathematical drivetrain model including gear shifting. This state space model is now extended by output equations in order to complete the plant model. The output equations are chosen in order to map the problem of smooth and lossless gear shifting to a common trajectory MIMO tracking problem.

A. Plant Model

Fig. 2 shows all possible states of a clutch and indicates the transitions between them. Since dissipation in clutches occurs exclusively in slipping state, this state has to be avoided in lossless gear shifting. According to Fig. 2 both releasing and locking of a clutch can be performed without intermediate slipping state. On the one hand a lossless transition from locked to released state is achieved, if the clutch torque τ_C, which is actually a locking torque $\tau_{C,lk}$, is zero, while decreasing p. The process of decreasing $\tau_{C,lk}$ to zero is called clutch unloading. On the other hand a lossless transition from released to locked state is achieved, if the differential angular velocity $\Delta\dot{\varphi}_C$ between the clutch plates is zero while increasing p. The process of decreasing $\Delta\dot{\varphi}_C$ to zero, is called clutch synchronization. If clutch unloading resp. synchronization is performed without any influence on the required angular velocity of the driving wheels $\dot{\varphi}_W$, the gear shift is done in the required optimal way. Since the calculation of both $\Delta\dot{\varphi}_C$ and $\tau_{C,lk}$ was already part of Chapter II [see (9) and (30)], the plant model for the gear shift $\boldsymbol{\kappa}_i \rightarrow \boldsymbol{\kappa}_j$ can be easily completed in state space for both cases:

1) Locking a clutch ($\boldsymbol{\kappa}_i^T \boldsymbol{\kappa}_i < \boldsymbol{\kappa}_j^T \boldsymbol{\kappa}_j$): In this case $\dot{\varphi}_W$ and $\Delta\dot{\varphi}_C = \Delta\boldsymbol{\kappa}_{i,j}^T \Delta\dot{\boldsymbol{\varphi}}_{C,i}$ [see (31) and (9)] have to be controlled. This leads to a MIMO LTI (linear time invariant) state space model:

$$\Sigma_{\boldsymbol{\kappa}_i}^{\boldsymbol{\kappa}_{j,lk}}: \ \dot{\mathbf{q}}_i = \underbrace{\bar{\mathbf{M}}_i^{-1}\bar{\mathbf{A}}_i}_{\mathbf{A}_i}\mathbf{q}_i + \underbrace{\bar{\mathbf{M}}_i^{-1}\bar{\mathbf{B}}_i}_{\mathbf{B}_i}\mathbf{u},$$
$$\mathbf{y}_i = \begin{bmatrix} y_1 \\ y_2 \end{bmatrix} = \begin{bmatrix} \dot{\varphi}_W \\ \Delta\dot{\varphi}_C \end{bmatrix} = \underbrace{\begin{bmatrix} \mathbf{e}_{\mathbf{q}_i}^T \\ \mathbf{c}_{i,lk}^T \end{bmatrix}}_{\mathbf{C}_{i,lk}}\mathbf{q}_i, \tag{32}$$

with $\mathbf{c}_{i,lk}^T = \bar{\mathbf{b}}_{C,i,lk} = \bar{\mathbf{B}}_{C,i}\Delta\boldsymbol{\kappa}_{i,j}$. Hereby $\mathbf{e}_{\mathbf{q}_i}^T$ is a vector of suitable length, selecting the angular velocity of the driving wheels from state vector $\mathbf{q}_i$.

2) Releasing a clutch ($\boldsymbol{\kappa}_i^T \boldsymbol{\kappa}_i > \boldsymbol{\kappa}_j^T \boldsymbol{\kappa}_j$): In this case $\dot{\varphi}_W$ and $\tau_{C,lk} = \Delta\boldsymbol{\kappa}_{i,j}^T \boldsymbol{\tau}_{C,i,lk}$ [see (31) and (30)] have to be controlled. Analogously to the above case this leads to a similar MIMO LTI state space model with a different output equation:

$$\Sigma_{\boldsymbol{\kappa}_i}^{\boldsymbol{\kappa}_{j,rl}}: \ \dot{\mathbf{q}}_i = \underbrace{\bar{\mathbf{M}}_i^{-1}\bar{\mathbf{A}}_i}_{\mathbf{A}_i}\mathbf{q}_i + \underbrace{\bar{\mathbf{M}}_i^{-1}\bar{\mathbf{B}}_i}_{\mathbf{B}_i}\mathbf{u},$$
$$\mathbf{y}_i = \begin{bmatrix} y_1 \\ y_2 \end{bmatrix} = \begin{bmatrix} \dot{\varphi}_W \\ \tau_{C,lk} \end{bmatrix} = \underbrace{\begin{bmatrix} \mathbf{e}_{\mathbf{q}_i}^T \\ \mathbf{c}_{i,rl}^T \end{bmatrix}}_{\mathbf{C}_{i,rl}}\mathbf{q}_i + \underbrace{\begin{bmatrix} \mathbf{0} \\ \mathbf{d}_{i,rl}^T \end{bmatrix}}_{\mathbf{D}_{i,rl}}\mathbf{u}, \tag{33}$$

with

$$\mathbf{c}_{i,rl}^T = -\left[\bar{\mathbf{b}}_{C,j,lk}^T \bar{\mathbf{M}}_j^{-1} \bar{\mathbf{b}}_{C,j,lk}\right]^{-1} \bar{\mathbf{b}}_{C,j,lk}^T \bar{\mathbf{M}}_j^{-1} \bar{\mathbf{A}}_j \mathbf{J}_{q_j,q_i},$$
$$\mathbf{d}_{i,rl}^T = -\left[\bar{\mathbf{b}}_{C,j,lk}^T \bar{\mathbf{M}}_j^{-1} \bar{\mathbf{b}}_{C,j,lk}\right]^{-1} \bar{\mathbf{b}}_{C,j,lk}^T \bar{\mathbf{M}}_j^{-1} \bar{\mathbf{B}}_{R,j}, \tag{34}$$

and $\bar{\mathbf{b}}_{C,j,lk} = \bar{\mathbf{B}}_{C,j}\Delta\boldsymbol{\kappa}_{i,j}$. Note that although the output equations refer to the $\mathbf{q}_i$-coordinates system, parameters $\mathbf{c}_{i,rl}^T$ and $\mathbf{d}_{i,rl}^T$ depend on the system parameters of the $\mathbf{q}_j$-coordinate system.

Since the slipping torques $\boldsymbol{\tau}_{C,sl}$ are avoided, in both cases the input vector is truncated to the propulsion torques:

$$\mathbf{u} := \boldsymbol{\tau}_P. \tag{35}$$

For sake of simplicity the further considerations assume drivetrain topologies offering two propulsion elements.

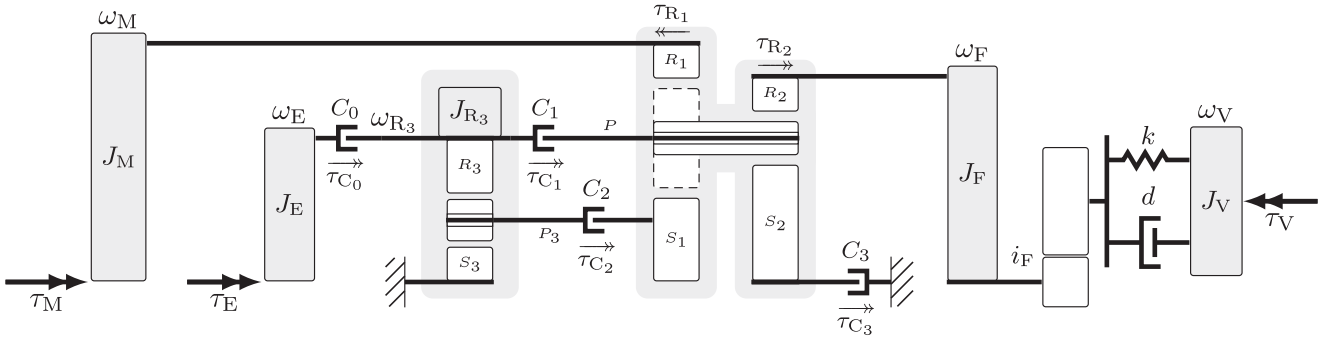

Fig. 3. Mechanical scheme of the exemplary hybrid electric drivetrain topology including an extended Ravigneaux planetary gear set with two separated ring gears (R_1 and R_2).

B. Control Problem Statement

Using the plant models $\Sigma_{\boldsymbol{\kappa}_i}^{\boldsymbol{\kappa}_{j,\mathrm{lk}}}$ and $\Sigma_{\boldsymbol{\kappa}_i}^{\boldsymbol{\kappa}_{j,\mathrm{rl}}}$ [see (32) and (33)] the general control task in smooth and lossless gear shifting can be stated as common MIMO tracking problem:

Steer y_2 to zero while y_1 tracks a smooth reference trajectory.

More general the task is to simultaneously track trajectories for both system outputs employing two control inputs. Since decoupling theory offers a necessary and sufficient condition to this task, its principles shall be shortly recapitulated: This so called decoupling problem, was first solved by Morgan in [30] who proposed a necessary condition for the existence of a static state feedback. Falb and Wolovich developed a necessary and sufficient condition to this problem in [31], considering the regularity of the corresponding decoupling matrix $\hat{\mathbf{D}}$.

1) Static State Decoupling of MIMO LTI Systems: Consider the following MIMO LTI system consisting of n states $\mathbf{x}$, m inputs $\mathbf{u}$ and m outputs $\mathbf{y}$:

$$\begin{aligned}\dot{\mathbf{x}} &= \mathbf{A}\mathbf{x} + \mathbf{B}\mathbf{u},\\ \mathbf{y} &= \mathbf{C}\mathbf{x} + \mathbf{D}\mathbf{u}.\end{aligned} \tag{36}$$

$\mathbf{A}, \mathbf{B}, \mathbf{C}$ and $\mathbf{D}$ are constant matrices of appropriate dimensions. The task is to evaluate the existence of a static state feedback,

$$\mathbf{u} = \mathbf{V}\mathbf{x} + \mathbf{K}\mathbf{w}, \tag{37}$$

that decouples the input-output behavior of the new inputs $\mathbf{w}$ to the outputs $\mathbf{y}$. This problem was first solved by Morgan in [30] who proposed a necessary condition for the existence of decoupling matrices $\mathbf{V}$ and $\mathbf{K}$. Falb and Wolovich developed a necessary and sufficient condition to this problem in [31]:

Theorem 1 (Existence of a decoupling static state feedback). A decoupling static state feedback law (37) exists, if and only if the decoupling matrix,

$$\hat{\mathbf{D}} = \begin{bmatrix} \hat{\mathbf{d}}_1^T \\ \vdots \\ \hat{\mathbf{d}}_m^T \end{bmatrix}, \quad \hat{\mathbf{d}}_i^T := \begin{cases} \mathbf{d}_i^T, & \text{for } \delta_i = 0 \\ \mathbf{c}_i^T \mathbf{A}^{\delta_i - 1}\mathbf{B}, & \text{for } \delta_i \neq 0, \end{cases} \tag{38}$$

is nonsingular.

Hereby δ_i is the relative degree of output y_i with respect to $\mathbf{u}$:

$$\delta_i := \min\left\{ j : \mathbf{c}_i^T \mathbf{A}^{j-1}\mathbf{B} \neq \mathbf{0},\ \ j = 1, 2, \ldots, n-1 \right\}. \tag{39}$$

The vectors $\mathbf{c}_i^T$ denotes the respective row in the output matrix $\mathbf{C}$.

This necessary and sufficient condition of Falb and Wolovich is used to state a condition for gear shifting: If, and only if, matrix $\hat{\mathbf{D}}$ (38) of the system $\Sigma_{\boldsymbol{\kappa}_i}^{\boldsymbol{\kappa}_{j,\mathrm{lk}}}$ resp. $\Sigma_{\boldsymbol{\kappa}_i}^{\boldsymbol{\kappa}_{j,\mathrm{rl}}}$ is nonsingular the system outputs $\mathbf{y}$ can be controlled independently. If so, consequently, it is possible to bring the differential angular velocity $\Delta\dot{\varphi}_{\mathrm{C}}$ of the locking clutch respectively the locking torque $\tau_{\mathrm{C,lk}}$ of the releasing clutch to zero, while simultaneously controlling rotational speed of the driving wheels. Therefore, this is a sufficient condition, if a required gear shift can be performed in a smooth and lossless way. The condition is sufficient but not necessary, since the avoidance of slipping just requires $\Delta\dot{\varphi}_{\mathrm{C}} = 0$ resp. $\tau_{\mathrm{C,lk}} = 0$ at the switching time. Obviously this is less restrictive than the above requirement of tracking a trajectory for $\Delta\dot{\varphi}_{\mathrm{C}}$ resp. $\tau_{\mathrm{C,lk}}$. However, considering robustness, meeting $\Delta\dot{\varphi}_{\mathrm{C}} = 0$ resp. $\tau_{\mathrm{C,lk}} = 0$ at the switching time is quite critical. Therefore, the sufficient condition is of major interest from the practical point of view. If this condition is not met, consequently, from the practical point of view, either dissipation in clutches or propulsion torque interruption has to by accepted in the considered gear shift. If this condition is met various control approaches can be applied on this common MIMO tracking problem.

IV. Exemplary Implementation of a Control System

The investigations of the above chapters are now applied to an exemplary multi-mode drivetrain topology. Furthermore, in Section IV-D a generic, model-based feedforward control for gear shifts in this topology is presented.

Fig. 3 shows a simplified mechanical scheme of a hybrid electric drivetrain topology as presented in [23].

It comprises an ICE as well as an electric motor with the propulsion torques τ_{E} and τ_{M}. The gearbox consists of an extended Ravigneaux planetary gear set $(\mathrm{S}_1, \mathrm{S}_2, \mathrm{P}, \mathrm{R}_1, \mathrm{R}_2)$, featuring two separated ring gears, and a single planetary gear set $(\mathrm{S}_3, \mathrm{P}_3, \mathrm{R}_3)$. For engagement of different transmission modes

it offers four clutches. Although clutch C_3 is actually a brake, it can be considered as common clutch in this application. The output of the gear box is connected to the driving wheels via a fixed transmission ratio i_F and a spring-damper-configuration (stiffness k and damping constant d), modeling a flexible shaft.

A. Linear Model

Since the mechanical scheme in Fig. 3 shows five inertias and one flexible shaft, according to Chapter II it is sufficient to use a state vector $\mathbf{x}$ of dimension $n = 6$ [cf. (4)]:

$$\mathbf{x} = \begin{bmatrix} \omega_\mathrm{E} & \omega_{\mathrm{R}_3} & \omega_\mathrm{M} & \omega_\mathrm{V} & i_\mathrm{F}^{-1} \cdot \varphi_\mathrm{F} - \varphi_\mathrm{V} & v \end{bmatrix}^T. \quad (40)$$

The first four elements of state vector $\mathbf{x}$ are angular velocities of inertias. The fifth state is the torsion (differential angular position) of the flexible shaft between gear box output and driving wheels. The last element is the vehicle's velocity v, since this quantity is of interest and in direct relation to the angular velocity of the driving wheels by the wheel radius r:

$$v = \omega_\mathrm{W} \cdot r. \quad (41)$$

The input vector $\mathbf{u}$ consists of propulsion torques $\boldsymbol{\tau}_\mathrm{P}$ (ICE and motor), vehicle reaction torque τ_V, and clutch torques $\boldsymbol{\tau}_\mathrm{C}$:

$$\mathbf{u}^T = [\underbrace{\tau_\mathrm{E} \quad \tau_\mathrm{M}}_{\boldsymbol{\tau}_\mathrm{P}^T} \quad \tau_\mathrm{V} \quad \underbrace{\tau_{\mathrm{C}0} \quad \tau_{\mathrm{C}1} \quad \tau_{\mathrm{C}2} \quad \tau_{\mathrm{C}3}}_{\boldsymbol{\tau}_\mathrm{C}^T}]. \quad (42)$$

With respect to the choice of state vector $\mathbf{x}$ in (40) the modeling approach presented in Chapter II leads to system matrices $\bar{\mathbf{M}}$, $\bar{\mathbf{A}}$, $\bar{\mathbf{B}}$:

$$\bar{\mathbf{M}} = \mathrm{diag}\left(\begin{bmatrix} J_\mathrm{E} & J_{R_3} & J_\mathrm{M} & J_\mathrm{F} & 1 & \frac{J_\mathrm{V}}{r^2} \end{bmatrix}\right).$$

$$\bar{\mathbf{A}} = \begin{bmatrix} -d_\mathrm{J} & 0 & 0 & 0 & 0 & 0 \\ 0 & -d_\mathrm{J} & 0 & 0 & 0 & 0 \\ 0 & 0 & -d_\mathrm{J} & 0 & 0 & 0 \\ 0 & 0 & 0 & -d_\mathrm{J} - \frac{d}{i_\mathrm{F}^2} & -\frac{k}{i_\mathrm{F}} & \frac{d}{r \cdot i_\mathrm{F}} \\ 0 & 0 & 0 & \frac{1}{i_\mathrm{F}} & 0 & -\frac{1}{r} \\ 0 & 0 & 0 & \frac{d}{r \cdot i_\mathrm{F}} & \frac{k}{r} & -\frac{d_\mathrm{J}+d}{r^2} \end{bmatrix}$$

$$\bar{\mathbf{B}} = \begin{bmatrix} \bar{\mathbf{B}}_\mathrm{P} & \bar{\boldsymbol{b}}_\mathrm{V} & \bar{\mathbf{B}}_\mathrm{C} \end{bmatrix}, \quad \text{with} \quad (43)$$

$$\bar{\mathbf{B}}_\mathrm{P} = \begin{bmatrix} 1 & 0 \\ 0 & 0 \\ 0 & 1 \\ 0 & 0 \\ 0 & 0 \\ 0 & 0 \end{bmatrix}, \quad \bar{\mathbf{B}}_\mathrm{C} = \begin{bmatrix} -1 & 0 & 0 & 0 \\ 1 & -1 & i_{\mathrm{P}3}^{\mathrm{R}3} & 0 \\ 0 & i_\mathrm{P}^{\mathrm{R}1} & i_{\mathrm{S}1}^{\mathrm{R}1} & i_{\mathrm{S}2}^{\mathrm{R}1} \\ 0 & i_\mathrm{P}^{\mathrm{R}2} & i_{\mathrm{S}1}^{\mathrm{R}2} & i_{\mathrm{S}2}^{\mathrm{R}2} \\ 0 & 0 & 0 & 0 \\ 0 & 0 & 0 & 0 \end{bmatrix}$$

$$\bar{\boldsymbol{b}}_\mathrm{V}^T = \begin{bmatrix} 0 & 0 & 0 & 0 & 0 & -\frac{1}{r} \end{bmatrix}$$

Damping constant d_J ensures slightly damped motion of all inertias. Transmission ratios $i_\mathrm{P}^{\mathrm{R}1}$, $i_\mathrm{P}^{\mathrm{R}2}$, $i_{\mathrm{P}3}^{\mathrm{R}3}$, $i_{\mathrm{S}1}^{\mathrm{R}1}$, $i_{\mathrm{S}1}^{\mathrm{R}2}$, $i_{\mathrm{S}2}^{\mathrm{R}1}$ and $i_{\mathrm{S}2}^{\mathrm{R}2}$ are defined by so-called Willis equations of the planetary gearsets. The interested reader is referred to [32]. Tables I and II list the parameter values used in the system matrices $\bar{\mathbf{M}}$, $\bar{\mathbf{A}}$ and $\bar{\mathbf{B}}$.

TABLE I
SYSTEM PARAMETERS

Symbol	Value	Unit
J_E	$64.0 \cdot 10^{-3}$	$\mathrm{kg \cdot m^2}$
$J_{\mathrm{R}3}$	$10.0 \cdot 10^{-3}$	$\mathrm{kg \cdot m^2}$
J_M	$32.5 \cdot 10^{-3}$	$\mathrm{kg \cdot m^2}$
J_F	$333.3 \cdot 10^{-3}$	$\mathrm{kg \cdot m^2}$
J_V	135.7	$\mathrm{kg\,m^2}$
d	20	$\mathrm{N\,m \cdot s}$
d_J	10^{-4}	$\mathrm{Nm \cdot s}$
k	$4 \cdot 10^3$	$\mathrm{N\,m}$
r	0.317	m

TABLE II
GEAR RATIOS

Symbol	Value
i_F	4.616
$i_\mathrm{P}^{\mathrm{R}1}$	0.260
$i_\mathrm{P}^{\mathrm{R}2}$	0.480
$i_{\mathrm{P}3}^{\mathrm{R}3}$	−0.676
$i_{\mathrm{S}1}^{\mathrm{R}1}$	−0.316
$i_{\mathrm{S}1}^{\mathrm{R}2}$	1.633
$i_{\mathrm{S}2}^{\mathrm{R}1}$	0.745
$i_{\mathrm{S}2}^{\mathrm{R}2}$	−0.491

TABLE III
MODE CLASSIFICATION

Clutch state κ				Mode	Gear	
c_0	c_1	c_2	c_3		Name	Index i
0	0	0	0	—	—	1
0	0	0	1	FM	E2	2
0	0	1	0	—	—	3
0	0	1	1	FM	E2	4
0	1	0	0	—	—	5
0	1	0	1	FM	E2	6
0	1	1	0	FM	E1	7
0	1	1	1	—	—	8
1	0	0	0	—	—	9
1	0	0	1	FM	E2	10
1	0	1	0	CV	CV1	11
1	0	1	1	FC	G1	12
1	1	0	0	CV	CV2	13
1	1	0	1	FC	G3	14
1	1	1	0	FC	G2	15
1	1	1	1	—	—	16

Since the exemplary hybrid electric drivetrain topology offers four clutches to set different transmission modes, a four-element clutch state vector $\boldsymbol{\kappa} = \begin{bmatrix} c_0 & c_1 & c_2 & c_3 \end{bmatrix}^T$ is introduced. Table III summarizes the possible transmission modes defined by the clutch states $\boldsymbol{\kappa}$. Hereby FM denotes a fixed transmission ratio from electric motor to gearbox output. In FC modes the propulsion torque can be split between engine and motor. The exemplary topology offers 3 FCs, 2 FMs and 2 CVs. According to Table III, there are 4 different clutch states to set E2. The remaining 6 possible clutch states do not represent a valid transmission mode (see Table III), since they either lock

the transmission ($i = 8, 16$) or do not enable power transfer to the gearbox output($i = 1, 3, 5, 9$).

According to Section II-B transformation matrices $\mathbf{J}_{\mathrm{x},\mathrm{q}_i}$ define the fixed relations between the rotational speeds of inertias due to a specific clutch state $\boldsymbol{\kappa}_i$. Since relations between the rotational speeds of the actuators' inertias and the gearbox output characterize the current transmission mode, the results listed in Table III can be directly obtained from the matrices $\mathbf{J}_{\mathrm{x},\mathrm{q}_i}$.

For the following considerations index i is restricted to the set $I = \{2, 4, 6, 7, 10, 11, 12, 13, 14, 15\}$, which represents all gears, i.e., clutch states with valid transmission mode according to Table III.

B. Gear Shifting Analysis

In order to apply the sufficient condition on smooth and lossless gear shifting presented in Chapter III, in a first step the relative degrees for every elementary gear shift have to be determined. Therefore, it is necessary to consider the output equations $y_1 = v$ and $y_2 = \Delta\dot{\varphi}_{\mathrm{C}}$ resp. $y_2 = \tau_{\mathrm{C,lk}}$ [see (32) and (33)] separately:

v : According to (39) the process of subsequent time derivation of the output equality can be stopped after the second derivation with respect to time:

$$\mathbf{e}_{\mathbf{q}_i}^T \bar{\mathbf{M}}_i^{-1} \bar{\mathbf{B}}_{\mathrm{P},i} = \mathbf{0}^T \qquad \forall i \in I$$
$$\mathbf{e}_{\mathbf{q}_i}^T \bar{\mathbf{M}}_i^{-1} \bar{\mathbf{A}}_i \bar{\mathbf{M}}_i^{-1} \bar{\mathbf{B}}_{\mathrm{P},i} \neq \mathbf{0}^T \qquad \forall i \in I$$
$$\Downarrow$$
$$\delta_{\mathrm{v}} = 2. \tag{44}$$

Since the considered topology offers two propulsion elements, $\mathbf{0}^T$ is a zero matrix of dimension (1×2). The results confirms the following physical interpretation: In every valid transmission mode, the propulsion torque of at least one actuator acts directly on the gearbox output. Consequently, the propulsion torque has to pass two serial inertias to influence vehicle velocity. Therefore, the relative degree has to be two.

$\Delta\dot{\varphi}_{\mathrm{C}}$: Input vector $\mathbf{u}$ appears for the first time in the first derivative with respect to time of the output equation. Therefore, the following inequality holds:

$$\left(\bar{\mathbf{B}}_{\mathrm{C},i}(\bar{\boldsymbol{\kappa}}_i)^T \bar{\mathbf{M}}_i^{-1} \bar{\mathbf{B}}_{\mathrm{P},i}\right)_k \neq \mathbf{0}^T \tag{45}$$
$$\forall i \in I, \qquad k = 1, \ldots, \bar{\boldsymbol{\kappa}}_i{}^T \bar{\boldsymbol{\kappa}}_i,$$

where $(\mathbf{A})_k$ is the k-th row of a matrix $\mathbf{A}$, $\bar{\boldsymbol{\kappa}}_i$ is the element-wise logical negation of $\boldsymbol{\kappa}_i$ and therefore $\bar{\mathbf{B}}_{\mathrm{C},i}(\bar{\boldsymbol{\kappa}}_i)$ denotes the selection of all non zero columns (according to still released clutches) in $\bar{\mathbf{B}}_{\mathrm{C},i}$. Consequently the relative degree of output $\Delta\dot{\varphi}_{\mathrm{C}}$ is:

$$\delta_{\mathrm{lk}} = 1. \tag{46}$$

This result can also be explained physically: As one can see in (43) every constraint due to a locked clutch involves at least one state which is directly influenced by an actuator. Therefore, the relative degree has to be one. Since locking a clutch reduces the number of mechanical degrees of freedom, it is obvious that $\delta_{\mathrm{lk}} = 1$ is valid for all gears.

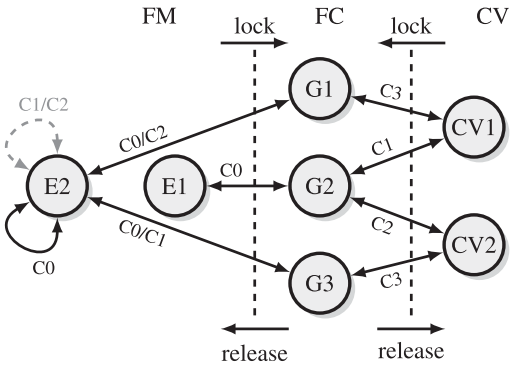

Fig. 4. Graphical representation of the gear shifting analysis.

$\tau_{\mathrm{C,lk}}$: According to (33) there is a direct feed-through in this output equation. Therefore the following inequality holds:

$$\Big(\left[\bar{\mathbf{B}}_{\mathrm{C},i}(\bar{\boldsymbol{\kappa}}_i)^T \bar{\mathbf{M}}_i^{-1} \bar{\mathbf{B}}_{\mathrm{C},i}(\bar{\boldsymbol{\kappa}}_i)\right]^{-1} \times \bar{\mathbf{B}}_{\mathrm{C},i}(\bar{\boldsymbol{\kappa}}_i)^T \bar{\mathbf{M}}_i^{-1} \bar{\mathbf{B}}_{\mathrm{P},i} \Big)_k \neq \mathbf{0}^T$$
$$\forall i \in I, \qquad k = 1, \ldots, \bar{\boldsymbol{\kappa}}_i{}^T \bar{\boldsymbol{\kappa}}_i. \tag{47}$$

Consequently the relative degree of output $\tau_{\mathrm{C,lk}}$ is:

$$\delta_{\mathrm{rl}} = 0. \tag{48}$$

Using the above results on relative degrees, the decoupling matrices for an elementary gear shift $\boldsymbol{\kappa}_i \rightarrow \boldsymbol{\kappa}_j$ with $i, j \in I$ are stated:

1) locking:

$$\hat{\mathbf{D}}_{\mathrm{lk}} = \begin{bmatrix} \mathbf{e}_{\mathbf{q}_i}^T \bar{\mathbf{M}}_i^{-1} \bar{\mathbf{A}}_i \bar{\mathbf{M}}_i^{-1} \bar{\mathbf{B}}_{\mathrm{P},i} \\ \bar{\mathbf{b}}_{\mathrm{C},i,\mathrm{lk}}^T \bar{\mathbf{M}}_i^{-1} \bar{\mathbf{B}}_{\mathrm{P},i} \end{bmatrix} \tag{49}$$

2) releasing:

$$\hat{\mathbf{D}}_{\mathrm{rl}} = \begin{bmatrix} \mathbf{e}_{\mathbf{q}_i}^T \bar{\mathbf{M}}_i^{-1} \bar{\mathbf{A}}_i \bar{\mathbf{M}}_i^{-1} \bar{\mathbf{B}}_{\mathrm{P},i} \\ \left[\bar{\mathbf{b}}_{\mathrm{C},j,\mathrm{lk}}^T \bar{\mathbf{M}}_j^{-1} \bar{\mathbf{b}}_{\mathrm{C},j,\mathrm{lk}}\right]^{-1} \bar{\mathbf{b}}_{\mathrm{C},j,\mathrm{lk}}^T \bar{\mathbf{M}}_j^{-1} \bar{\mathbf{B}}_{\mathrm{P},j} \end{bmatrix} \tag{50}$$

If the decoupling matrices in (49) resp. (50) are non-singular, the gear shift $\boldsymbol{\kappa}_i \rightarrow \boldsymbol{\kappa}_j$ can be performed in the required way. The evaluation of the regularity of all possible decoupling matrices according to all possible gear shifts in the exemplary topology is illustrated in Fig. 4. Solid arrows denote the possibility to perform a smooth and lossless gear shift, i.e., the corresponding decoupling matrix is regular. Dashed arrows denote gear shifts which can be exclusively performed accepting either dissipation in clutches or propulsion torque interruption, i.e., the corresponding decoupling matrix is singular. The arrow labels show the corresponding clutches that have to be locked resp. released. As one can see in Fig. 4 all gears are connected by solid arrows in a closed network. Therefore, it is in principle possible to perform all gear shifts in a smooth and lossless way, but the number of necessary interim gears may not be minimal.

C. Exemplary Gear Shifts

This section shows an exemplary implementation of a generic control strategy for gear shifting. The proposed implementation covers gear shifts between FCs (G1,G2,G3):

$$\boldsymbol{\kappa}_i \rightarrow \boldsymbol{\kappa}_j, \quad \text{with:} \quad i,j \in \{12,14,15\}, \quad i \neq j. \tag{51}$$

In stationary driving these gears play an essential role, since they enable direct control of the battery's state of charge (SOC). The considered gear shifts are non-elementary, since

$$\Delta\boldsymbol{\kappa}_{i,j}^T \Delta\boldsymbol{\kappa}_{i,j} = 2 \neq 1 \quad \forall i,j \in \{12,14,15\}, \quad i \neq j. \tag{52}$$

For $\Delta\boldsymbol{\kappa}_{i,j}$ see (31). However, it is possible to split these gear shifts into a series of two elementary gear shifts ($\boldsymbol{\kappa}_i \rightarrow \boldsymbol{\kappa}_m$, $\boldsymbol{\kappa}_m \rightarrow \boldsymbol{\kappa}_j$) by introducing an interim gear $\boldsymbol{\kappa}_m$:

$$\boldsymbol{\kappa}_m = \boldsymbol{\kappa}_i \wedge \boldsymbol{\kappa}_j. \tag{53}$$

(The symbol $\wedge$ denotes the element-wise logical conjunction.) Evaluation of (53) to all possible gear shifts according to (51) delivers the set of possible interim gears:

$$m \in \{10,11,13\}. \tag{54}$$

This results can be easily proofed considering Fig. 4 and Table III. From the mathematical point of view the gear shift $\boldsymbol{\kappa}_i \rightarrow \boldsymbol{\kappa}_j$ involves three dynamical systems:

$$\Sigma_{\boldsymbol{\kappa}_i} \rightarrow \Sigma_{\boldsymbol{\kappa}_m} \rightarrow \Sigma_{\boldsymbol{\kappa}_j}. \tag{55}$$

Hereby the following relation between generalized coordinates $\mathbf{q}_i$, $\mathbf{q}_m$ and $\mathbf{q}_j$ holds:

$$\mathbf{q}_m = \mathbf{J}_{\mathbf{q}_m,\mathbf{q}_i}\mathbf{q}_i = \mathbf{J}_{\mathbf{q}_m,\mathbf{q}_j}\mathbf{q}_j. \tag{56}$$

In order to perform these gear shifts in the required way, in a first step the clutch determined by $\Delta\boldsymbol{\kappa}_{i,m}$ has to be released:

$$\Delta\boldsymbol{\kappa}_{i,m} = \boldsymbol{\kappa}_i \veebar \boldsymbol{\kappa}_m \quad \left(\Delta\boldsymbol{\kappa}_{i,m}^T \Delta\boldsymbol{\kappa}_{i,m} = 1\right). \tag{57}$$

In a second step the clutch determined by $\Delta\boldsymbol{\kappa}_{m,j}$ is locked:

$$\Delta\boldsymbol{\kappa}_{m,j} = \boldsymbol{\kappa}_m \veebar \boldsymbol{\kappa}_j \quad \left(\Delta\boldsymbol{\kappa}_{m,j}^T \Delta\boldsymbol{\kappa}_{m,j} = 1\right). \tag{58}$$

D. Shift Procedure and Control Phases

The considered gear shift is embedded into a stationary driving situation. Therefore, five control phases arise:

1) *Phase I – Stationary Driving*
   Since the current gear i (clutch state $\boldsymbol{\kappa}_i$) is a FC, the required propulsion power can be split between ICE and motor. The Hybrid Control Unit (HCU) demands a specific torque split, with respect to the battery's SOC. Consequently, the control task in phase I is to set this demanded torque split. Phase I ends as the gear shift command occurs.
2) *Phase II – Clutch Unloading*
   Initiated by the gear shift command, in phase II the lossless releasing of a clutch is prepared. Therefore, the locking torque of the respective clutch is steered to zero, following a smooth trajectory. The fully unloaded clutch can be released without dissipation.
3) *Phase III – Clutch Synchronization*
   In phase III the drivetrain operates in the intermediate gear m (clutch state $\boldsymbol{\kappa}_m$). In order to finish the gear shift, another clutch has to be locked. If the respective differential angular velocity is synchronized, dissipation is avoided. Therefore, it is steered to zero, following a smooth trajectory.
4) *Phase IV – Torque Split Recovery*
   In phase IV the gear shift is already finished in terms of the final gear j (clutch state $\boldsymbol{\kappa}_j$) is active. Nevertheless, the actual torque split differs from the torque split demanded by the HCU, and consequently has to be recovered smoothly. This implies smooth loading of the clutch, which has been locked.
5) *Phase V – Stationary Driving*
   Back in stationary driving, the gear shift is completely finished. Consequently, this last phase possibly coincides with phase I of another gear shift.

During all control phases the vehicle velocity follows a smooth reference trajectory defined by the driver via the accelerator pedal. Fig. 5 illustrates the introduced control phases. It further shows the the respective plant models, according to Section III-A. Note that systems $\Sigma^{\mathrm{v}}_{\boldsymbol{\kappa}_i}$ resp. $\Sigma^{\mathrm{v}}_{\boldsymbol{\kappa}_j}$ are SISO (single-input-single-output) systems:

$$\Sigma^{\mathrm{v}}_{\boldsymbol{\kappa}_{i/j}} : \dot{\mathbf{q}}_{i/j} = \mathbf{A}_{i/j}\mathbf{q}_{i/j} + \mathbf{b}_{\mathrm{P}}\tau_{\mathrm{P}}, \tag{59}$$

$$y = v = \mathbf{e}_{\mathbf{q}_{i/j}}^T \mathbf{q}_{i/j}.$$

τ_{P} is the superposition of the impacts of τ_{E} and τ_{M} on the system, therefore $\mathbf{b}_{\mathrm{P}} = \begin{bmatrix} 1 & 0 & 0 \end{bmatrix}^T$. For the MIMO systems $\Sigma^{\boldsymbol{\kappa}_{m,\mathrm{rl}}}_{\boldsymbol{\kappa}_i}$, $\Sigma^{\boldsymbol{\kappa}_{j,\mathrm{lk}}}_{\boldsymbol{\kappa}_m}$, and $\Sigma^{\boldsymbol{\kappa}_{m,\mathrm{rl}}}_{\boldsymbol{\kappa}_j}$ see (33) and (32).

At this point a comparison to the phases of an existing standard shift procedure is reasonable. For this comparison a classical power up-shift ($i_{\mathrm{new}} < i_{\mathrm{old}}$ and $\tau_{\mathrm{P}} > 0$) procedure of DCTs (see for example [7] and [33]), which is applied similarly in multi-mode (hybrid) transmissions, is selected. This gear shift equivalently shifts from one fixed transmission ratio to another and consists of mainly two phases: Decreasing the pressure on the releasing (off-going) clutch initiates the first phase, called *torque phase*. The hydraulic pressure on the second, on-coming, clutch is simultaneously increased in order to hand over the propulsion torque. When the second clutch, which is still slipping, transmits the full torque, the pressure is further increased in order to synchronize the engine speed to the new gear. This phase is called *inertia phase*. In most shifting strategies the engine torque is used to support this synchronization. The shift ends when the on-coming clutch transitions into locking state.

In the presented shifting procedure the torque phase is actually separated into clutch unloading phase and torque split recovery (clutch loading) phase and in between synchronization phase is inserted. The propulsion torque is not directly handed over from the off-going to the on-coming clutch, but transfered to an alternative transmission path, which does not include both clutches. This fact enables lossless shifting. The inertia phase corresponds to the clutch synchronization phase in the presented shifting procedure. The main difference is that the synchronization is done exclusively by the ICE and the electric motor,

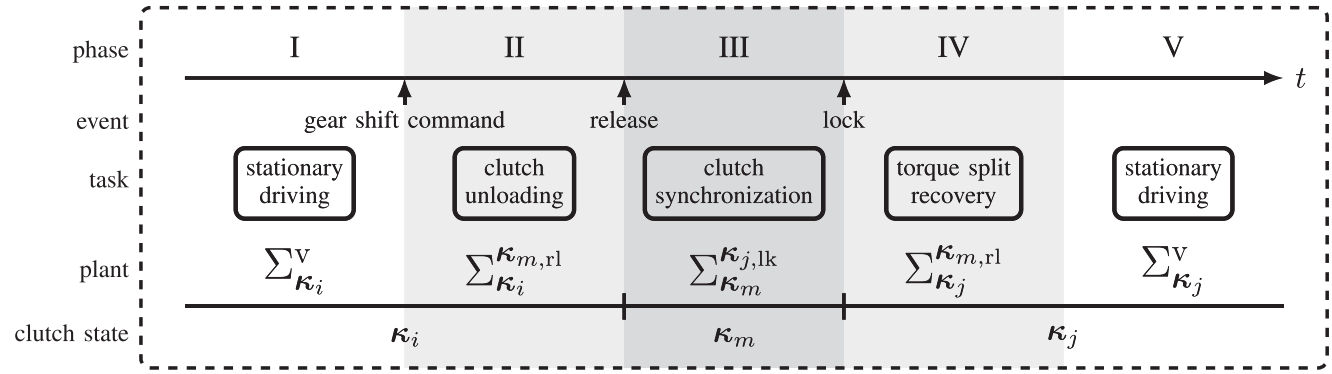

Fig. 5. Control phases for the smooth and lossless gear shift $\boldsymbol{\kappa}_i \rightarrow \boldsymbol{\kappa}_j$ embedded into a stationary driving situation (see Section IV-D).

avoiding the use of slipping torque at off-going or on-coming clutch. Note that furthermore a multi clutch actuation scenario (multi element shifting) is avoided and one of the most critical points in standard shift procedures — clutch transitions between slipping and locking — does not cause difficulties (cf. section IV-G). In standard shift procedures one has to distinguish in general first between up- and down-shifts ($i_{\mathrm{new}} < i_{\mathrm{old}}$ resp. $i_{\mathrm{new}} > i_{\mathrm{old}}$): In the case of a down-shift the inertia phase takes place before the torque phase, since otherwise acceleration of the engine speed would cause decrease of the propulsion torque. Furthermore, standard shift procedures distinguish between power and coast shifts ($\tau_{\mathrm{P}} > 0$ resp. $\tau_{\mathrm{P}} < 0$), again affecting the order of the shifting phases.

In contrast, the presented approach uses the same sequence of phases for all four shifting cases. This advantage definitely supports simplicity in the application. Furthermore, the presented shifting procedure offers easy handling of change-of-mind-scenarios, initiated for example by the driver's torque request. Clutch unloading can be aborted and withdrawn simply, by recovering original torque split. A change-of-mind occurring during synchronization phase is handled by changing the synchronizing clutch and restarting the phase in order to perform the shift back to the original fixed transmission ratio. Therefore, no additional functionalities are needed in these scenarios.

Although the main features of a standard shift procedure can still be recognized, this comparison emphasizes the novelty of the presented shifting procedure.

E. Feed Forward Control System Design

In this section control laws are designed, in order to handle the control phases stated in Section IV-D (see Fig. 5). A classical feedforward approach is applied: The necessary propulsion torques to track a required output behavior are calculated by inverting the dynamical input-output-behavior of the respective systems. To avoid causality problems this calculation employs derivatives of the reference trajectories. The implementation of the single feedforward control laws is now considered in more detail.

1) Phase I - Stationary Driving: According to Section IV-D the control task in this phase is to meet on the one hand the required vehicle velocity and on the other hand a demanded torque split between ICE and motor. Due to the fixed ratio of the actuators' angular velocities, in FCs the transfer functions ($\tau_{\mathrm{E}} \rightarrow y_{\mathrm{V}}$ and $\tau_{\mathrm{M}} \rightarrow y_{\mathrm{V}}$) differ only by a constant factor:

$$G_{i,\mathrm{E/M}}(s) = \frac{v(s)}{\tau_{\mathrm{E/M}}(s)} = \mathbf{e}_{q_i}^T \left(s\mathbf{I}_i - \mathbf{A}_i\right) \mathbf{b}_{i\mathrm{E/M}}$$

$$= \bar{b}_{i,\mathrm{E/M}} \bar{V}_i \frac{\left(s + \frac{k}{d}\right)}{\mathbf{a}_i^T \mathbf{s}_3}. \tag{60}$$

$\mathbf{I}_i$ is an identity matrix of proper dimension. Vector $\mathbf{a}_i$ assembles the denominator polynomial's coefficients and vector $\mathbf{s}_3$ the powers of the complex variable s beginning from zero up to the power of 3, which is the length of vector $\mathbf{a}_i$:

$$\mathbf{a}_i = \begin{bmatrix} a_{i,0} & a_{i,1} & a_{i,2} & 1 \end{bmatrix}^T, \tag{61}$$
$$\mathbf{a}_i^T \mathbf{s}_3 = s^3 + a_{i,2}s^2 + a_{i,1}s + a_{i,0}.$$

Parallel paths of action lead to zeros in the according transfer functions. Therefore, there is a LHS (left hand side) zero at $-\frac{k}{d}$ in the transfer function in (60) due to the parallel spring damper configuration of the flexible shaft. The structure of the transfer function in (60) offers a simple possibility to implement a feedforward control law meeting the required vehicle velocity, while providing the demanded torque split. In a first step the constant $\bar{b}_{i,\mathrm{E/M}}$ is neglected in order to calculate the overall propulsion torque τ_{P} to meet the required vehicle acceleration by using model inversion:

$$\tau_{\mathrm{P}}(s) = \mathbf{G}_{i,\mathrm{P}}^{-1} w_{\mathrm{v}}(s),$$

$$\mathbf{G}_{i,\mathrm{P}}^{-1}(s) = \frac{\mathbf{a}_i^T \mathbf{s}}{\left(s + \frac{k}{d}\right)} \bar{V}_i^{-1}. \tag{62}$$

The enumerator polynomial of (62) is calculated algebraically by usage of trajectory $w_{\mathrm{v}}(t)$ and its derivatives. According to the relative degree of the transfer function, it would sufficient to guarantee that trajectory $w_{\mathrm{v}}(t)$ is twice differentiable. A further restriction to three times differentiable trajectories at this point will later show its benefit. Vector $\mathbf{w}_{\mathrm{v}}$ contains the trajectory and its derivatives:

$$\mathbf{w}_{\mathrm{v}} = \begin{bmatrix} w_{\mathrm{v}} & \dot{w}_{\mathrm{v}} & \ddot{w}_{\mathrm{v}} & \dddot{w}_{\mathrm{v}} \end{bmatrix}^T. \tag{63}$$

The denominator polynomial of (62) is applied by filtering. Without the restriction to three times differentiable trajectories, one zero of the inverse transfer function $\mathbf{G}_i^{-1}(s)$ has to be

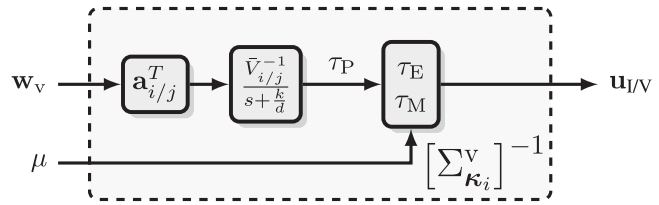

Fig. 6. Feedforward control structure to phase I and V: Stationary driving [see (62) and (64)].

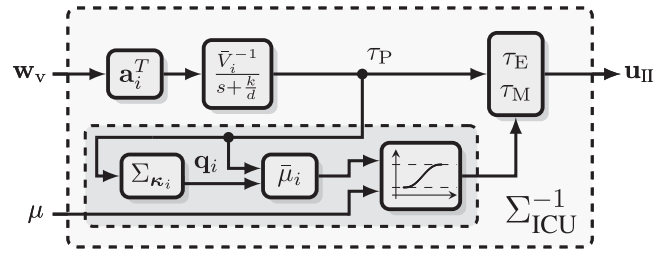

Fig. 7. Extension of feedforward control structure in phase I for application in phase II: Implicit Clutch Unloading [see Fig. 6 and (66) and (67)].

included into the filter, which would still lead to a proper filter transfer function. In a next step τ_P is split to τ_E and τ_M:

$$\tau_\mathrm{E} = \tau_\mathrm{P} \cdot \frac{\mu}{\bar{b}_{i,\mathrm{E}}}, \quad \tau_\mathrm{M} = \tau_\mathrm{P} \cdot \frac{1-\mu}{\bar{b}_{i,\mathrm{M}}}. \tag{64}$$

Factor μ defines a certain torque split between the actuators, from $\mu = 1$ (only combustion engine) to $\mu = 0$ (only electric motor). For $\mu > 1$ the electric motor is operated as generator. In this case the combustion engine has to provide more power than necessary for the required propulsion. μ is demanded by the HCU. Fig. 6 illustrates the simple structure of the feedforward control scheme.

2) Phase II - (Implicit) Clutch Unloading: In phase II an implicit clutch unloading (ICU) approach is applied. Hereby the torque split μ is modified in order to unload the releasing clutch. Although this approach differs from the direct clutch unloading strategy ($\tau_{\mathrm{C,lk}} \to 0$) in notation, the effect to the system is equivalent. The relation between the requirement $\tau_{\mathrm{C,lk}} = 0$ at the clutch $\Delta\boldsymbol{\kappa}_{i,m}$ and a specific torque split $\bar{\mu}_i$ is calculated using (64) in (33):

$$\tau_{\mathrm{C,lk}} = \mathbf{c}_{i,\mathrm{rl}}^T \mathbf{q}_i + \mathbf{d}_{i,\mathrm{rl}}^T \begin{bmatrix} \frac{\bar{\mu}_i}{\bar{b}_{i,\mathrm{E}}} & \frac{1-\bar{\mu}_i}{\bar{b}_{i,\mathrm{M}}} \end{bmatrix}^T \tau_\mathrm{P} \overset{!}{=} 0 \tag{65}$$

$$\Rightarrow \bar{\mu}_i = \frac{\frac{\mathbf{c}_{i,\mathrm{rl}}^T \mathbf{q}_i}{\tau_\mathrm{P}} - \frac{d_{i,\mathrm{M}}}{\bar{b}_{i,\mathrm{M}}}}{\frac{d_{i,\mathrm{E}}}{\bar{b}_{i,\mathrm{E}}} - \frac{d_{i,\mathrm{M}}}{\bar{b}_{i,\mathrm{M}}}}, \quad \text{with} \quad \mathbf{d}_{i,\mathrm{rl}}^T = \begin{bmatrix} d_{i,\mathrm{E}} & d_{i,\mathrm{M}} \end{bmatrix} \tag{66}$$

According to (66) to every given driving situation ($\tau_\mathrm{P} \neq 0$ and $\mathbf{q}_i$), exists a unique torque split $\bar{\mu}_i$, which fully unloads the respective clutch $\Delta\boldsymbol{\kappa}_{i,m}$. Smooth transition from actual torque split μ to $\bar{\mu}_i$, consequently, implicitly unloads the clutch. Therefore, feedforward control of phase I (see Fig. 6) just needs to be slightly extended, for application in phase II (see Fig. 7). Propulsion torque τ_P is calculated in the feedforward control of phase I. $\mathbf{q}_i$ can be obtained from a dynamical model $\Sigma_{\boldsymbol{\kappa}_i}$:

$$\Sigma_{\boldsymbol{\kappa}_i} : \dot{\mathbf{q}}_i = \mathbf{A}_i \mathbf{q}_i + \mathbf{b}_\mathrm{P} \tau_\mathrm{P}. \tag{67}$$

Since, consistent initialization of $\Sigma_{\boldsymbol{\kappa}_i}$ in (67) with respect to the actual system states is critical to the determination of $\bar{\mu}$, alternatively, an observer as suggested in [34] would achieve more robust results.

The benefit of implicit clutch unloading is, that explicit model inversion of the plant model in this phase is avoided, which is indicated by the following renaming:

$$\left[\Sigma_{\boldsymbol{\kappa}_i}^{\boldsymbol{\kappa}_{m\,,\mathrm{rl}}}\right]^{-1} \mapsto \Sigma_\mathrm{ICU}^{-1}. \tag{68}$$

3) Phase III - Clutch Synchronization: In phase III there are two control tasks: tracking of a required vehicle velocity trajectory ($v \overset{!}{=} w_\mathrm{v}$) and steering the differential angular velocity between the clutch plates of the locking clutch to zero ($\Delta\dot{\varphi}_\mathrm{C} \to 0$). Section IV-B proofs the possibility to meet both control tasks simultaneously by actuating the ICE and the motor. The input-output-behavior of the system $\Sigma_{\boldsymbol{\kappa}_m}^{\boldsymbol{\kappa}_{j,\mathrm{lk}}}$ can be considered in frequency domain, introducing transfer matrix $\mathbf{G}_m(s)$:

$$\mathbf{G}_m(s) = \frac{\mathbf{y}_m(s)}{\mathbf{u}(s)} = \mathbf{C}_{m,\mathrm{rl}} \left(s\mathbf{I}_m - \mathbf{A}_m\right) \mathbf{B}_{m,\mathrm{P}}. \tag{69}$$

Inversion of transfer matrix $\mathbf{G}_m(s)$ enables the determination of a feedforward control:

$$\begin{aligned} \mathbf{u}(s) &= \mathbf{G}_m^{-1}(s)\mathbf{w}(s), \\ \mathbf{w}(s) &= \begin{bmatrix} w_\mathrm{v}(s) & w_\mathrm{lk}(s) \end{bmatrix}^T, \\ \mathbf{G}_m^{-1}(s) &= \begin{bmatrix} V_{m,11} \frac{\mathbf{a}_{m\,,11}^T \mathbf{s}_3}{\left(s+\frac{k}{d}\right)} & V_{m,12} \mathbf{a}_{m,12}^T \mathbf{s}_1 \\ V_{m,21} \frac{\mathbf{a}_{m\,,21}^T \mathbf{s}_3}{\left(s+\frac{k}{d}\right)} & V_{m,22} \mathbf{a}_{m,22}^T \mathbf{s}_1 \end{bmatrix}. \end{aligned} \tag{70}$$

Whereas the relation of the vectors $\mathbf{a}_{m,12}$ and $\mathbf{a}_{m,22}$ to the system parameters in (43) can easily be stated, the far more complicate relation to the vectors $\mathbf{a}_{m,11}$ and $\mathbf{a}_{m,21}$ are analytically not considered in more detail:

$$\mathbf{a}_{m,12} = \begin{bmatrix} \frac{2d_\mathrm{J}}{J_\mathrm{E}+J_{\mathrm{R}\,3}} & 1 \end{bmatrix}^T, \tag{71}$$

$$\mathbf{a}_{m,22} = \begin{bmatrix} \frac{d_\mathrm{J}}{J_\mathrm{M}} & 1 \end{bmatrix}^T. \tag{72}$$

Fig. 8 shows the corresponding feedforward control scheme.

Analogously to phase I and II, three derivatives of vehicle velocity trajectory $w_\mathrm{v}(t)$ are applied, although in principal only two derivatives would be necessary. The feedforward control needs an additional trajectory $w_\mathrm{lk}(t)$ for the differential angular velocity $\Delta\dot{\varphi}_\mathrm{C}$ and its first derivative.

$$\mathbf{w}_\mathrm{lk} = \begin{bmatrix} w_\mathrm{lk} & \dot{w}_\mathrm{lk} \end{bmatrix}^T \tag{73}$$

In order to achieve continuous actuation signals, it is mandatory to choose the trajectory's initial values $\mathbf{w}_{\mathrm{lk,II\text{-}III}} = \begin{bmatrix} w_{\mathrm{lk,II\text{-}III}} & \dot{w}_{\mathrm{lk,II\text{-}III}} \end{bmatrix}$ consistent to the actual values at the switching time between phase II and III. These values can be provided

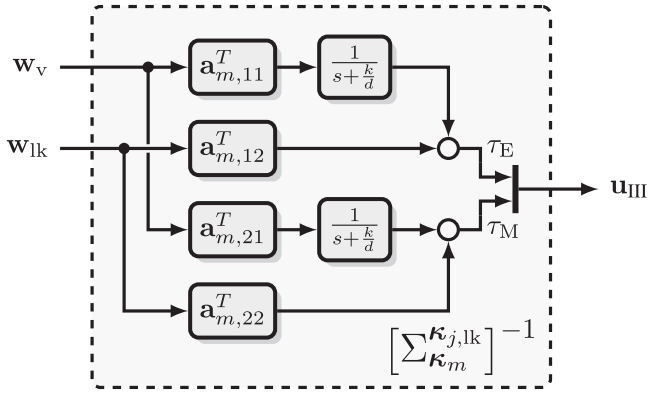

Fig. 8. Feedforward control structure to phase III: Clutch Synchronization [see (70)–(72)].

by system $\tilde{\Sigma}_{\boldsymbol{\kappa}_i}$:

$$\tilde{\Sigma}_{\boldsymbol{\kappa}_i}: \dot{\mathbf{q}}_i = \mathbf{A}_i\mathbf{q}_i + \mathbf{b}_\mathrm{P}\tau_\mathrm{P}$$
$$\mathbf{y} = \begin{bmatrix} \mathbf{c}^T_{i,\mathrm{lk}} \\ \mathbf{c}^T_{i,\mathrm{lk}}\mathbf{A}_i \end{bmatrix}\mathbf{q}_i + \begin{bmatrix} \mathbf{0} \\ \mathbf{c}^T_{i,\mathrm{lk}}\mathbf{b}_\mathrm{P} \end{bmatrix}\tau_\mathrm{P}. \tag{74}$$

At this point once again an observer can increase robustness. The final values of trajectory $w_\mathrm{lk}(t)$ and its derivatives have to fulfill:

$$\mathbf{w}_{\mathrm{lk,III\text{-}IV}} = \begin{bmatrix} w_{\mathrm{lk,III\text{-}IV}} & \dot{w}_{\mathrm{lk,III\text{-}IV}} \end{bmatrix}^T \stackrel{!}{=} \mathbf{0}^T. \tag{75}$$

In order to obtain not only continuous, but continuously differentiable actuation signals, it is possible at this point to include the second derivative with respect to time into the trajectory planning for $w_\mathrm{lk}(t)$. Note that this is only possible, if the vehicle velocity trajectory $w_\mathrm{v}(t)$ is restricted to be three times differentiable (cf. Section IV-E1), since $\dot{\mathbf{u}}$ is needed to determine the additional initial value. This approach is applied in the simulations in Section IV-I.

4) Phase IV - Torque Split Recovery (TSR): In phase IV the transition of the actual torque split $\bar{\mu}_j$ resulting from phase III to the torque split μ, demanded by the HCU, has to be controlled. Discontinuities in the actuation signals are avoided, if this transition is performed smoothly. In analogy to phase II, this approach can be called implicit clutch loading, since it implies smoothly increasing the torque transmitted on the locked clutch. At this point the relation between the actuation signals $\mathbf{u}_\mathrm{III}$ and the resulting torque split $\bar{\mu}_j$ in FC j (clutch state $\boldsymbol{\kappa}_j$) needs to be investigated. $\bar{\mu}_j$ is related to the ratio between the power of the engine and the motor:

$$\frac{P_\mathrm{E}}{P_\mathrm{M}} = \frac{\tau_\mathrm{E}\omega_\mathrm{E}}{\tau_\mathrm{M}\omega_\mathrm{M}} = \frac{\bar{\mu}_j}{1-\bar{\mu}_j} \quad \Rightarrow \quad \bar{\mu}_j = \bar{\mu}_j(\mathbf{x},\mathbf{u}). \tag{76}$$

According to the transformation matrix $\mathbf{J}_{\mathbf{q}_j}$, the ratio between the rotational speed of ICE and motor in FC gears is constant:

$$\mathbf{J}_{\mathbf{q}_j} = \begin{bmatrix} i_{\mathrm{E},j} & i_{\mathrm{E},j} & i_{\mathrm{M},j} & 1 & 0 & 0 \\ 0 & 0 & 0 & 0 & 1 & 0 \\ 0 & 0 & 0 & 0 & 0 & 1 \end{bmatrix}^T \quad \Rightarrow \quad \frac{\omega_{\mathrm{E},j}}{\omega_{\mathrm{M},j}} = \frac{i_{\mathrm{E},j}}{i_{\mathrm{M},j}}. \tag{77}$$

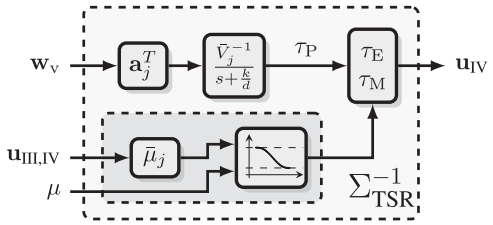

Fig. 9. Extension of feedforward control structure in phase V for application in phase IV: Torque Split Recovery [see Fig. 6 and (78)].

Therefore, torque split factor $\bar{\mu}_j$ does not depend on the rotational speeds of the actuators:

$$\bar{\mu}_j = \frac{\tau_\mathrm{E}\cdot\frac{i_{\mathrm{E},j}}{i_{\mathrm{M},j}}}{\tau_\mathrm{M}+\tau_\mathrm{E}\cdot\frac{i_{\mathrm{E},j}}{i_{\mathrm{M},j}}} = \bar{\mu}_j(\mathbf{u}). \tag{78}$$

Evaluation of (78) at the transition time between phase III and IV ($\rightarrow \mathbf{u}_\mathrm{III,IV}$) determines the actual torque split, which is the initial value for the smooth transition. Fig. 9 shows the feedforward control structure for this control task. It extends the feedforward control structure of phase V in Fig 6. Analogously to phase II, explicit inversion of the plant model in this phase is avoided. This is indicated by the renaming:

$$\left[\Sigma^{\boldsymbol{\kappa}_{m,\mathrm{rl}}}_{\boldsymbol{\kappa}_j}\right]^{-1} \mapsto \Sigma^{-1}_\mathrm{TSR}. \tag{79}$$

5) Phase V - Stationary Driving: To control the stationary driving situation of FC j (clutch state $\boldsymbol{\kappa}_j$) the feedforward control structure of FC i (clutch state $\boldsymbol{\kappa}_i$) can be reused (see Fig. 6).

F. Polynomial Trajectory Planning

In order to create the required trajectories a polynomial approach is used:

$$w(t) = \sum_{i=0}^{2n+1} a_i t^i \tag{80}$$

Variable n denotes the highest derivative $w^{(n)}(t)$, which is constrained by initial and final conditions (see for example (78)). All these conditions set up a system of linear equations of dimension $2n+2$, which determines the coefficients $a_0,\ldots a_{2n+1}$. The analytic expression enables straight forward calculation of corresponding extrema. These extrema are significant for the compliance for actuator magnitude and rate limits, which will be discussed in Section IV-I.

G. Clutch Actuation

In this exemplary application infinitely fast clutch actuation is assumed. This simplification enables increasing pressure p on the clutch plates from zero to the maximal pressure instantly. Due to this assumption, the instants of time when the clutch actuation is initiated and when the change of clutch states actually occurs, always coincide. If finite actuation time of clutches is considered, it is necessary to control the differential angular velocity resp. the locking torque to zero during the clutch actuation. In practice this duration is determined by the dynamics of the electro-hydraulic clutch actuation. However, it is also

possible to start clutch actuation simultaneously to the clutch unloading resp. the torque split recovery. To avoid premature releasing resp. locking, it is necessary to keep the maximal clutch torque according to the actual hydraulic pressure above the actual clutch torque. Since the value of the actual clutch torque is equal to the value of the corresponding trajectory (analytic polynomial) in the nominal case, this does not arise difficulties.

H. Compensation of Vehicle Reaction Torque

In Chapter II the vehicle reaction torque τ_v due to rolling resistance, air drag, and road gradient was introduced as disturbance input. For a known vehicle velocity the impact of this torque on the control tasks can be calculated and compensated by the propulsion torques τ_E and τ_M.

I. Simulation Setup and Results

The functionality of the presented control strategy is shown in simulation. To validate the presented modeling approach for simulation a drivetrain model suggested in [23] is implemented. This model has been validated in several applications. The model uses a slightly different modeling approach, than presented in Section II. The Lagrangian multipliers (locking torques) are explicitly calculated [cf. (15)] and treated as input torques in (13). Therefore, the order of the differential equation system is constant and independent of $\boldsymbol{\kappa}$. But, beside $\boldsymbol{\kappa} = \mathbf{0}$, the order is not minimal with respect to the system's mechanical degrees of freedom. Consequently, it contains redundant differential equations. Additionally, this model uses a clutch state logic to determine the actual clutch states.

The presented shift procedure is applied to control two different gear shifts, while accelerating the vehicle from 10 m/s to 20 m/s. The control phases II (implicit clutch unloading) and IV (torque split recovery) are planned to last 0.2 s, phase III (clutch synchronization) is planned to last 0.3 s. The simulation results are illustrated in Figs. 10 and 11.

Both simulations show the intended results: The gear shifts are performed without dissipation, since the releasing clutch is fully unloaded before releasing (first light gray area) and the locking clutch is synchronized before locking (dark gray area). Furthermore, shifting is performed smoothly, since the vehicle velocity perfectly tracks the polynomial trajectory. Also the second derivative of the vehicle velocity — the vehicle jerk — does not show any deviation from the required trajectory. Consequently, there is no additional jerk caused by the shifting. The clutch states, offered by the used drivetrain model, proof that actual clutch transitions take place at the intended time. The gear shift is finished after smooth torque split recovery (second light gray area). The torque split factor μ in the second simulation shows, that it is temporarily necessary to operate the electric motor regeneratively to meet the control tasks. Therefore, the signs of the rotational speed ω_M and torque τ_M are different in this period.

As already mentioned in Section IV-F the relation between the trajectories and actuation torques (τ_E and τ_M) shall now be investigated. These investigations are only valid for a constant driving situation, since the changing driver demands obviously

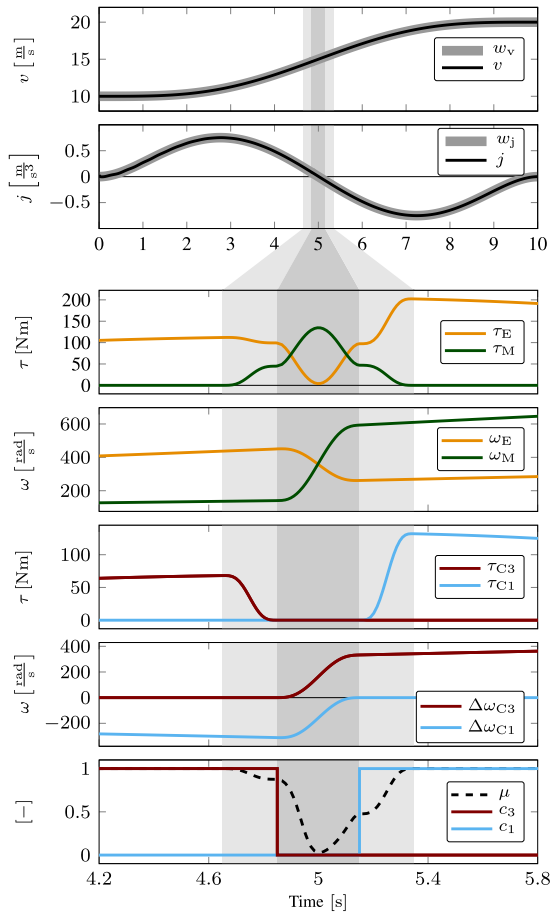

Fig. 10. Shift simulation 1: $\boldsymbol{\kappa}_{12} \rightarrow \boldsymbol{\kappa}_{15}$. This shift requires releasing clutch C_3 and locking clutch C_1 (see Fig. 4). In the stationary driving situation (before and after the gear shift) the combustion engine fully provides propulsion power ($\mu = 1$). During the shift the vehicle is accelerated from 10 m/s to 20 m/s.

impact the required actuation torques. Anyhow these investigations can be seen as reasonable estimations. During the clutch unloading phase the actuation torques are proportional to the trajectory for the torque split, i.e., the locking torque of the releasing clutch. Since (66) determines the torque split to fully unload the releasing clutch, it is possible to predict the courses of the actuation torques in advance. Therefore, it is possible to check on the one hand in advance, if the actuators can supply the final value. On the other hand the maximum torque rate can be decreased by prolonging the duration of this phase in order to comply the actuator constraints. The same consideration can be applied at the start of torque split recovery phase. Without proof in the clutch synchronization phase the actuation torques (τ_E and τ_M) are proportional to the first time derivative of the corresponding trajectory (differential angular velocity of the locking clutch). This enables decrease of both the maximal required torque value and rate in order to meet the actuator limits by prolonging the phase duration. Summarized, the information, if a certain shift can be performed in smooth and lossless manner within the actuator limits, and furthermore the minimal duration of the single phases can be precalculated. Table IV assembles the maxima and minima in value and slope of the single phases. This information is of special interest for the HCU, since it can

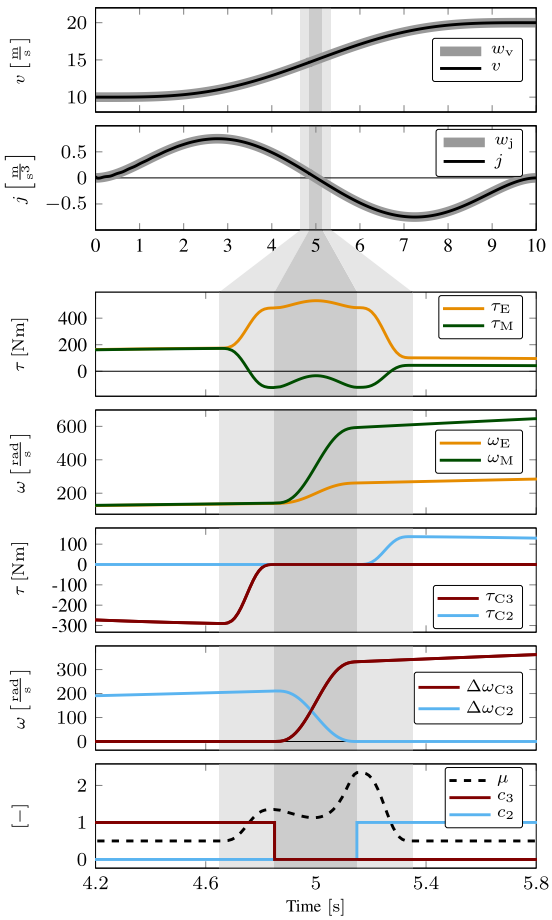

Fig. 11. Shift simulation 1: $\boldsymbol{\kappa}_{14} \rightarrow \boldsymbol{\kappa}_{15}$. This shift requires releasing clutch C_3 and locking clutch C_2 (see Fig. 4). In the stationary driving situation (before and after the gear shift) propulsion power is equally split between the combustion engine and the electric motor ($\mu = 0.5$) . During the shift the vehicle is accelerated from 10 m/s to 20 m/s.

TABLE IV
ACUTATION LIMITS

Phase	Limits	
	$\tau_{\max}$ resp. $\tau_{\min}$	$\dot{\tau}_{\max}$ resp. $\dot{\tau}_{\min}$
II	b	$\sim \frac{1}{T}$
III	$\sim \frac{1}{T}$	$\sim \frac{1}{T^2}$
IV	b	$\sim \frac{1}{T}$

b . . . maximum/minimum at boundary
T . . . duration of the corresponding phase

be considered within the general shift strategy. This point is a major benefit and consequently contribution of the presented combination of smart trajectory planing and feedforward control. Since the drivetrain topology is a stable plant, the second advantage is that the proposed structure can be easily extended by a feedback loop resulting in a classical Internal Model Control (IMC) structure (see [35] and [36]). This extensions ensures robustness according to model uncertainties and disturbances a by consecutive re-planing of the trajectories.

V. CONCLUSION AND OUTLOOK

This paper considers gear shifting in modern multi-mode transmission topologies on a new level of quality and performance. It focuses on a new general, systematic approach to model and control these smooth and lossless gear shifts. The first contribution is the systematic determination of a set of generalized coordinates and the corresponding model transformation in state space according to one or several locked clutches. Secondly, this paper contributes the general control problem statement of smooth and lossless gear shifting in state space. This representation supports the application of various control techniques. Thirdly, based on an exemplary multi-mode transmission, a novel shifting procedure for performing smooth and lossless gear shifts is proposed. The main advantages of this procedure are on the one hand its invariance to the actual driving situation (no differentiation between power/coast up/down-shifts), and on the other hand the simple handling of change-of-mind scenarios. Additionally, a feed forward approach is applied to control the shift procedure, featuring several advantages: A multi clutch actuation is avoided and clutch transitions, which are critical in standard shift procedures, can be handled easily. Polynomial trajectory planning enables analytic expressions for the actuation torques in the nominal case for constant driving situations. Therefore, violation of limits in magnitude and slope are avoided or at least predicted.

The promising first simulation results substantiate the continuing research on this topic to provide a generic, model-based control strategy for real-time application in automotive transmission control units, including discretization and validation in a demonstrator car.

REFERENCES

[1] A. Serrarens, M. Dassen, and M. Steinbuch, "Simulation and control of an automotive dry clutch," in *Proc. Amer. Control Conf.*, Jun. 2004, vol. 5, pp. 4078–4083.
[2] Z. Zhong, G. Kong, Z. Yu, X. Xin, and X. Chen, "Shifting control of an automated mechanical transmission without using the clutch," *Int. J. Automotive Technol.*, vol. 13, no. 3, pp. 487–496, 2012.
[3] M. Pettersson and L. Nielsen, "Gear shifting by engine control," *IEEE Trans. Control Syst. Technol.*, vol. 8, no. 3, pp. 495–507, May 2000.
[4] F. Garofalo, L. Glielmo, L. Iannelli, and F. Vasca, "Smooth engagement for automotive dry clutch," in *Proc. 40th IEEE Conf. Decis. Control*, 2001, vol. 1, pp. 529–534.
[5] C. H. Yu, C. Y. Tseng, and C. P. Wang, "Smooth gear-change control for EV clutchless automatic manual transmission," in *Proc. IEEE/ASME Int. Conf. Adv. Intell. Mechatronics*, Jul. 2012, pp. 971–976.
[6] K. van Berkel, T. Hofman, A. Serrarens, and M. Steinbuch, "Fast and smooth clutch engagement control for dual-clutch transmissions," *Control Eng. Pract.*, vol. 22, pp. 57–68, 2014.
[7] T. Szabo, M. Buchholz, and K. Dietmayer, "Optimal control of a gearshift with a dual-clutch transmission," in *Proc. ASME Dyn. Syst. Control Conf.*, 2011, pp. 1–6.
[8] L. Chen, G. Xi, and J. Sun, "Torque coordination control during mode transition for a series-parallel hybrid electric vehicle," *IEEE Trans. Veh. Technol.*, vol. 61, no. 7, pp. 2936–2949, Sep. 2012.
[9] F. Zhu, C. Yin, L. Chen, and C. Wang, "Design and analysis of a novel-multimode transmission for a HEV using a single electric machine," *IEEE Trans. Veh. Technol.*, vol. 62, no. 3, pp. 1–9, Mar. 2013.
[10] R. Isermann, *Elektronisches Management motorischer Fahrzeugantriebe (in German)*. New York, NY, USA: Springer-Verlag, 2010.
[11] W. Duan, F. Yan, and C. Du, "Powertrain control strategies overview for hybrid electric vehicles," in *Proc. 2010 Asia-Pac. Power Energy Eng. Conf.*, Mar. 2010, pp. 1–5.

[12] R. Gasper, R. Beck, P. Drews, and D. Abel, "Feedforward control of a parallel hybrid launch clutch," in *Proc. Eur. Control Conf. Budapest, Hungary*, 2009, pp. 4265–4270.
[13] R. Gasper and D. Abel, "Flatness based control of a parallel hybrid drivetrain," *Proc. 6th IFAC Symp. Adv. Automotive Control, Schwabing, Germany*, 2010, pp. 2943–2948.
[14] R. Gasper, F. Hesseler, and D. Abel, "Control of a parallel hybrid drivetrain: A flatness based approach," IFAC Proc. Vol., vol. 18, pp. 2943–2948, 2011.
[15] H.-D. Lee, S.-K. Sul, H.-S. Cho, and J.-M. Lee, "Advanced gear-shifting and clutching strategy for a parallel-hybrid vehicle," *IEEE Ind. Appl. Mag.*, vol. 6, no. 6, pp. 26–32, Nov. 2000.
[16] K. Li, J. Sun, X. Liu, and C. Zhang, "Torque coordinated control of PHEV based on the fuzzy and sliding mode method with load torque observer," in *Proc. 33rd Chin. Control Conf.*, Jul. 2014, pp. 7933–7937.
[17] R. C. Baraszu and S. R. Cikanek, "Torque fill-in for an automated shift manual transmission in a parallel hybrid electric vehicle," in *Proc. Amer. Control Conf.*, May 2002, vol. 2, pp. 1431–1436.
[18] R. Beck *et al.*, "Model predictive control of a parallel hybrid vehicle drivetrain," in *Proc. 44th IEEE Conf. Decis. Control*, 2005, pp. 2670–2675.
[19] R. Fischer, "Dedicated hybrid transmission (DHT) the new hybrid transmission category," in *Proc. 2015 CTI Symp.*, Dec. 2015.
[20] L. W. Tsai and G. Schultz, "A motor-integrated parallel hybrid transmission," *J. Mech. Des.*, vol. 126, no. 5, pp. 889–894, 2004.
[21] H. Zhang, Y. Zhang, and C. Yin, "Hardware-in-the-loop simulation of robust mode transition control for a series-parallel hybrid electric vehicle," *IEEE Trans. Veh. Technol.*, vol. 65, no. 3, pp. 1059–1069, Mar. 2016.
[22] S. Saenger-Zetina, K. Neiss, R. Beck, and P. D.-I. D. Abel, "Optimal clutch control applied to a hybrid electric variable transmission with kane equations," *IFAC Proc. Vol.*, vol. 40, no. 10, pp. 87–94, 2007.
[23] M. Bachinger, M. Stolz, and M. Horn, "A novel drivetrain modelling approach for real-time simulation," *Mechatronics*, vol. 32, pp. 67–78, 2015.
[24] H. Goldstein, C. Poole, and J. Safko, *Classical Mechanics*, 3rd ed. Reading, MA, USA: Addison-Wesley, 2002.
[25] W. Schiehlen, "Multibody system dynamics: Roots and perspectives," *Multibody Syst. Dyn.*, vol. 1, no. 2, pp. 149–188, 1997.
[26] C. D. Meyer, Ed., *Matrix Analysis and Applied Linear Algebra*. Philadelphia, PA, USA: SIAM, 2000.
[27] L. Glielmo, L. Iannelli, V. Vacca, and F. Vasca, "Gearshift control for automated manual transmissions," *IEEE/ASME Trans. Mechatronics*, vol. 11, no. 1, pp. 17–26, Feb. 2006.
[28] C. Lv, J. Zhang, and Y. Li, "Extended-Kalman-filter-based regenerative and friction blended braking control for electric vehicle equipped with axle motor considering damping and elastic properties of electric powertrain," *J. Veh. Syst. Dyn.*, vol. 54, pp. 1372–1388, Aug. 2014.
[29] C. Lv, J. Zhang, Y. Li, and Y. Yuan, "Mode-switching-based active control of a powertrain system with non-linear backlash and flexibility for an electric vehicle during regenerative deceleration," in *Proc. Inst. Mech. Eng., Part D, J. Automobile Eng.*, vol. 229, no. 11, pp. 1429–1442, 2015.
[30] B. Morgan, "The synthesis of linear multivariable systems by state-variable feedback," *IEEE Trans. Autom. Control*, vol. 9, no. 4, pp. 405–411, Oct. 1964.
[31] P. L. Falb and W. A. Wolovich, "Decoupling in the design and synthesis of multivariable control systems," NASA Techn. Note D-4219, Oct. 1967.
[32] H. Müller, W. Mannhardt, and J. Glover, *Epicyclic Drive Trains: Analysis, Synthesis, and Applications*. Detroit, MI, USA: Wayne State Univ. Press, 1982.
[33] R. Fischer, F. Kücükay, G. Jürgens, R. Najork, and B. Pollak, *The Automotive Transmission Book*. New York, NY, USA: Springer-Verlag, 2015.
[34] M. Bachinger, M. Stolz, and M. Horn, "Fixed time-step drivetrain observer for embedded automotive applications," in *Proc. IEEE Conf. Control Appl.*, 2014, pp. 47–52.
[35] M. Morari and E. Zafiriou, *Robust Process Control*. Englewood Cliffs, NJ, USA: Prentice-Hall, 1989.
[36] D. Schwarzmann, *Nonlinear Internal Model Control with Automotive Applications*. Bristol, CT, USA: ISD, 2008.

Johannes Rumetshofer received the M.Sc. degree in electrical engineering from Graz University of Technology, Graz, Austria, in 2015. He is currently working toward the Ph.D. degree in electrical engineering from the Institute of Automation and Control, Graz University of Technology.

In 2016, he joined the Control Systems Group, Department of Electrics/Electronics and Software, Virtual Vehicle Research Center, Graz, Austria. His current research interests include the modeling and control of automotive drivetrains.

Markus Bachinger received the M.Sc. and Ph.D. degrees in electrical engineering from Graz University of Technology, Graz, Austria, in 2001 and 2016, respectively. He was a development Engineer for diesel and exhaust aftertreatment control at AVL List GmbH, Graz, Austria, from 2001 to 2011. In 2011, he changed to Virtual Vehicle Research Center, Graz, Austria, elaborating his Ph.D. thesis within a funded cooperation project on the topic of real-time transmission modeling and control at the Institute of Automation and Control, Graz University of Technology. Since 2016, he technically leads the Transmission Controls Department at AVL List GmbH.

Michael Stolz received the M.Sc. degree in mechanical engineering and the Ph.D. degree in electrical engineering from Graz University of Technology, Graz, Austria, in 2002 and 2013, respectively.

He worked for six years in automotive industry as development engineer for diesel control at AVL-List GmbH. In 2009, he changed to the Virtual Vehicle Research Center elaborating his Ph.D. thesis within a founded cooperation project on the topic of diesel control at the Institute of Automation and Control, Graz University of Technology. Since 2014, he has been responsible for the control systems group in the Department of Electrics/Electronics and Software at the Virtual Vehicle Research Center. His main working areas include control oriented real time modeling, automotive control and control architectures, and automated driving.

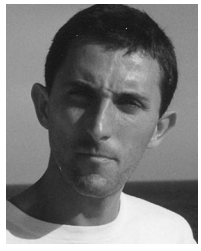

Martin Horn (M'07) received the Dipl.Ing. and Ph.D. degrees in electrical engineering from Graz University of Technology, Graz, Austria, in 1992 and 1998, respectively.

Until 2008, he was Associate Professor in the Institute of Automation and Control, Graz University of Technology. From 2008 to 2014, he was in the Institute for Smart System Technologies, Klagenfurt University, Austria, as a Professor of control and measurement systems. In 2014, he joined the Graz University of Technology, Austria, where he is currently a Professor of control and automation. His research interests include the fields of variable-structure systems, modeling and control of mechatronic systems, and automotive control systems.